Plant Physiology and Biochemistry 221 (2025) 109570

Contents lists available at ScienceDirect

Plant Physiology and Biochemistry

journal homepage: www.elsevier.com/locate/plaphy

Arabidopsis thaliana accumulates dehydroepiandrosterone after infection with phytopathogenic fungi – Effects on plants and fungi

Ceren Oktay [a], Glendis Shiko [a], Maximilian Liebl [b], Felix Feistel [c], Sarah Mußbach [a], Karl Ludwig Körber [a], Emanuel Barth [d], Ludwig Huber [b], Anna Antony [a], Ralf Oelmüller [a], Michael Reichelt [c], Kilian Ossetek [e], Christoph Müller [b], Alexandra C.U. Furch [a], Jan Klein [a,*]

[a] Plant Physiology, Matthias Schleiden Institute for Genetics, Bioinformatics and Molecular Botany, Friedrich Schiller University Jena, 07743, Jena, Germany
[b] Department of Pharmacy, Center for Drug Research, Ludwig-Maximilians-Universität München, 81377, Munich, Germany
[c] Department for Biochemistry, Max Planck Institute for Chemical Ecology, 07743, Jena, Germany
[d] Bioinformatics Core Facility, Friedrich Schiller University Jena, 07743, Jena, Germany
[e] Research Group Plant Defense Physiology, Max Planck Institute for Chemical Ecology, 07743, Jena, Germany

ARTICLE INFO

Keywords:
Arabidopsis thaliana
Alternaria brassicicola
Dehydroepiandrosterone
Mammalian steroids
Fungal infection
Ergosterol biosynthesis
Cell membrane integrity

ABSTRACT

Progestogens and androgens have been found in many plants, but little is known about their physiological function. We used a previously established UPLC-ESI-MS/MS method to analyze progestogen and androgen profiles in fungal infections. Here we show that dehydroepiandrosterone (DHEA), a C_{19} steroid, specifically accumulates in shoots of *Arabidopsis thaliana* (L.) HEYNH. infected with *Alternaria brassicicola* (SCHWEIN.) WILTSHIRE. Elevated DHEA levels in plants seem not to be product of fungal sterol/steroid precursor activity, but an intrinsic plant response to the infection. DHEA was applied exogenously to analyze the effects of the androgen on development and gene expression in *A. thaliana*. Our findings reveal that DHEA treatment down-regulates membrane-associated, salicylic acid and abscisic acid-regulated, as well as stress-responsive genes. Notably, DHEA does not inhibit the isoprenoid or post-lanosterol pathway of the ergosterol biosynthesis. Moreover, *A. brassicicola* was also treated with DHEA to analyze the growth, sterol pattern and membrane-integrity. Our data suggest that DHEA enhances the permeability of plant and fungal biomembranes. We propose that DHEA accumulation is a plant defense response which reduces fungal growth in plant tissues.

1. Introduction

Plants are threatened by phytopathogenic fungi in natural environments and agricultural ecosystems (Stukenbrock and McDonald, 2008). Therefore, it is not surprising that fungal phytopathogens destroy 30% of all farm plant products through diseases and spoilage. Moreover, mycotoxin-producing fungi endanger the safety of plant products produced for human or animal consumption (Avery et al., 2019).

Alternaria species are globally spread, necrotic pathogens (Jindo et al., 2021). They cause various diseases on multiple crops (Rotem, 1998). Infection by these fungi, which cause early blight, led to yield losses of 35–78% in tomatoes and 5–40% in potatoes (Grigolli et al., 2011). In *brassica* species, *Alternaria* species cause the *Alternaria* blight. According to the Food and Agriculture Statistics of the United Nations (FAOSTAT), edible brassicas are a major vegetable crop in 5th place in food production (Nowakowska et al., 2019). Moreover, brassicas are, except for soybean, the largest oil seed crop (Gupta, 2016). Therefore, 15–70% yield loss caused by *Alternaria* blight is economically harmful and endangers human nutrition (Nowakowska et al., 2019). *Alternaria* species sporulate best in an atmosphere with elevated CO_2 concentrations (Wolf et al., 2010). Therefore, the spread of fungal-caused plant diseases by climatic changes is to be feared (Al-Askar et al., 2014). *A. brassicicola* is an aggressive soil-borne pathogen. The first symptoms of infections are small brown to black spots often observed on older leaves of infected plants. Later, spots develop into irregularly shaped lesions, forming concentric rings. Yellow shadows often surround these rings (Nowicki et al., 2012). *Alternaria* produces mycotoxins, which can be split into three structural different groups: dibenzopyrone derivatives, the perylene derivative altertoxins, and tenuazonic acid. These

* Corresponding author.
E-mail address: jan.klein@uni-jena.de (J. Klein).

https://doi.org/10.1016/j.plaphy.2025.109570
Received 5 July 2024; Received in revised form 6 January 2025; Accepted 25 January 2025
Available online 28 January 2025

Abbreviations:

DHEA	dehydroepiandrosterone
SA	salicylic acid
ABA	abscisic acid
KC	ketoconazole

fungicides leads to accelerated developments of pathogen resistance and is a threat to natural environments (Fernández-Ortuño et al., 2008). Exemplarily: During the last 20 years the average use of pesticides per hectar in Germany increased from 2.98 kg in the year 2000 to 3.80 kg in 2019 (Schanzer et al., 2022). This results in the application of 30,000 tons of 285 different legally approved pesticides only in Germany in the year 2018 (Schanzer et al., 2021). Therefore, it is not surprising that *Alternaria* species developed resistance against widely used quinone outside inhibitors (e.g., pyraclostrobin) and succinate dehydrogenase

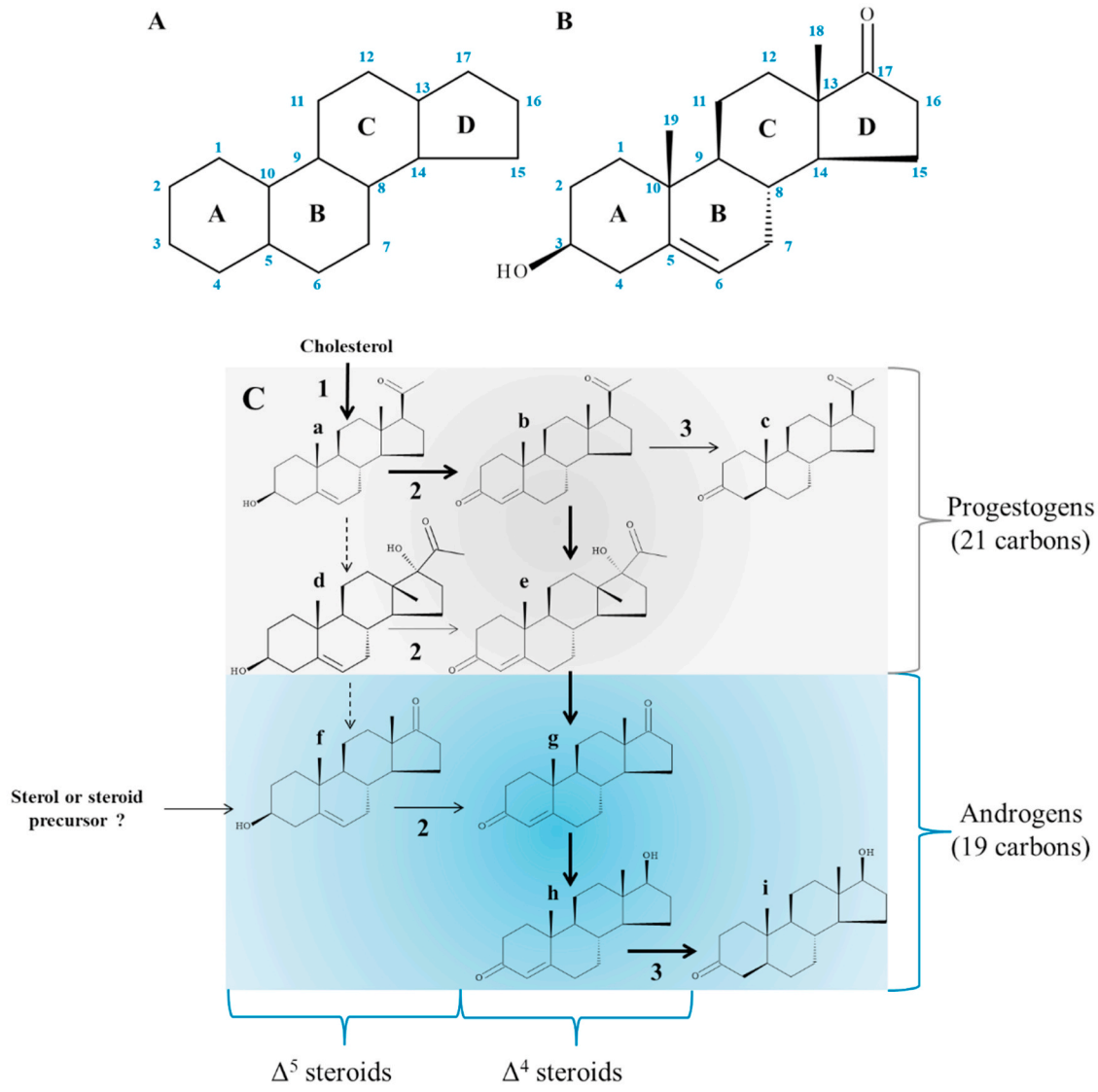

Fig. 1. Structure of steroids and the conversion of steroids in plants – a theory of plant steroidogenesis (Shiko et al., 2023**).** Steroids are tetracyclic triterpenoids with a sterane skeleton. This Figure depicts the sterane skeleton (**A**) of steroids. In dehydroepiandrosterone (**B**), the sterane skeleton is additionally substituted with a methyl group at C10 and C13, a hydroxyl group at C3, and an oxo moiety on C17, while a double bond connects C5 and C6. Carbon numbering and ring annotation follow IUPAC. (**C**) Findings of Shiko et al. (2023) show that reaction steps from mammal steroidogenesis are conserved in plants. Bold arrows depict the reaction steps of mammal steroidogenesis that could be found in all analyzed plants. It was suggested that androgen biosynthesis in plants favors a route using the Δ^4 pathway, which is described by an early conversion of Δ^5 into Δ^4 steroids (pregnonolone **a** into progesterone **b**). The analyzed steroids are abbreviated with the following letters (pregnenolone **a**; progesterone **b**; 5α-dihydroprogesterone **c**; 17α-hydroxypregnenolone **d**; 17α-hydroxyprogesterone **e**; dehydroepiandrosterone **f**; androstenedione **g**; testosterone **h**; 5α-dihydrotestosterone **i**). The identified enzymes of plant steroidogenesis are included as numbers (sterol side chain-cleavage enzyme **1**; 3β-hydroxysteroid dehydrogenase and ketosteroid isomerase **2**; steroid 5α-reductases **3**).

toxins can be detected in human food products such as tomatoes, apples, and cereals (Pinto and Patriarca, 2017).

Adding to the problem, the excessive use of giant amounts of inhibitors (e.g., boscalid; Nottensteiner et al., 2019).

Therefore, a large unmet need exists to develop new pest management strategies. Steroids, produced by plants or pathogens, control

many developmental, physiological, or growth processes, and especially the role of endogenous C_{21}- (progestogens) and C_{19}- (androgens) steroids in plants have not yet be sufficiently explored (Janeczko, 2021). It was shown that progestogens and androgens are widespread within the plant kingdom (Simons and Grinwich, 1989; Shiko et al., 2023). Shiko and colleagues (2023) identified dehydroepiandrosterone (DHEA; Fig. 1), a C_{19} steroid, in 85 % of the analyzed plants, from green algae to angiosperms.

Moreover, plants have been shown to convert steroids in a conserved way. Plants can perform all enzymatic reactions of mammalian steroidogenesis, including 3β- and 17β-hydroxysteroid dehydrogenase activity, 5α- and 5β-reduction of Δ^4 steroids, as well as 17α-hydroxylation and 17,20-lyase reactions. These findings were used to build a hypothetical biosynthesis pathway similar to the canonical mammalian steroidogenesis (Shiko et al., 2023, Fig. 1).

It has been shown for several plant species that treatment with progesterone, a progestogen, enhances resistance against several (a)biotic stresses (Genisel et al., 2013; Janeczko et al., 2013; Hao et al., 2019; Sabzmeydani et al., 2020; reviewed in: Klein, 2024). Moreover, the expression of the bovine CYP11A1, an enzyme that converts cholesterol into pregnenolone, in tomato and tobacco results in enhanced values of pregnenolone and progesterone. Consequently, these plants show enhanced resistance against the fungal pathogen *Botrytis cinerea* (Shpakovski et al., 2017). This raises the question if endogenous steroids participate in pathogen response in *A. thaliana*. Within this study, we analyzed the profiles of endogenous C_{21}- and C_{19}-steroids in *A. thaliana* shoots after infection with *A. brassicicola*. We could detect that DHEA-levels are elevated in infected shoots, while other changes of the steroid levels were not detected. This indicates a role of DHEA in plant infections with fungal pathogens. Therefore, we analyzed the effects of DHEA on plants and the fungal pathogen *A. brassicicola*.

2. Material and methods

2.1. Plant material

10-day-old seedlings of *A. thaliana* (L.) HEYN. Col. 0 (*A. thaliana*) cultivated on MS-medium (Murashige and Skoog, 1962) were transferred to poor nutrient medium (PNM; Camehl et al., 2011) consisting of 5 mM KNO_3, 2 mM $MgSO_4$, 2 mM $Ca(NO_3)_2$, 0.01 μM $FeSO_4$, 70 μM H_3BO_3, 14 μM $MnCl_2$, 0.5 μM $CuSO_4$, 1 μM $ZnSO_4$, 0,2 μM Na_2MoO_4, 0.01 μM $CoCl_2$, 10.5 g L^{-1} agar (pH 5.6). *Spirodela polyrhiza* clone 9509 was prepared from the stock collection of the Friedrich Schiller University Jena and cultivated on a sugar-free nutrient medium for *Lemnaceae* according to Appenroth et al. (1996, 2018). *Hordeum vulgare* cv. Avalon was obtained from Petra Sandjohann (Gut Obbach Schäfer GbR, Euerbach-Obbach, Germany) and cultivated as described before (Shiko et al., 2023).

2.2. Fungus cultivation

Alternaria brassicicola SCHWEIN. WILTSHIRE was cultivated in potato dextrose agar (PDA; pH = 6.5–6.8; Carl Roth GmbH, Germany) in the dark at 28 °C for 4 weeks. Plates were used for further experiments.

2.3. Infection of plants with A. brassicicola

10 mL of isolation solution (0.01% Tween-20 in sterile water) was added to well-grown fungal mycelium on the PDA plates. The suspended mycelium was carefully removed from the surface of the PDA agar surface. The fungal solution was filtered through 4 layers of nylon membrane (SEFAR NITEX 03–70; fibre material: PA 6.6, monofilament; mesh opening: 70 ± 4 μM; mesh count: 81 n cm^{-1}; Sefar AG, Heiden, Switzerland). Spores were pelletized by centrifuging for 1 min at 12,000 *g* at 22 °C and resuspended in new isolation solution. This was repeated 4 times. The concentration of the spore solution was adjusted to 1×10^6 spores per mL using a hemocytometer. For infection of *A. thaliana* or *S. polyrhiza*, 2 μL of spore solution was applied onto a single leaf.

2.4. Microscopy

Leaves of *S. polyrhiza* or Rhodamine stained hyphae of *A. brassicicola* were mounted on a glass slide with a cover slip for microscopic inspection using an Axio Imager.M2 (Zeiss Microscopy GmbH, Jena, Germany) equipped with a 10x objective (N-Achroplan 10×/0.3). Bright-field images were recorded with a monochromatic camera: Axiocam 503 mono (Zeiss Microscopy GmbH). Fluorescence images (EX 545/25 and EM 605/70) were recorded with a color camera: Axiocam 503 color (Zeiss Microscopy GmbH, Jena) by use of DsRED filter (605/70 nm). Digital images were processed with the ZEN software (Zeiss Microscopy GmbH), treated with Adobe® PhotoShop to optimize brightness, contrast and coloring.

2.5. Analysis of A. brassicicola growth and spore production influenced by DHEA

To analyze the effects of DHEA on fungal growth, a plug of well-grown *A. brassicicola* mycelium (d = 5 mm) was transferred to PDA plates supplemented with 3–30 μM DHEA dissolved in DMSO, while pure DMSO was used for control treatment. The diameter of the grown colony was analyzed after 14 days.

To analyze spore production, 20 μL of spore solution (see above) was spread onto a PDA plate supplemented with DHEA; after 14 days, spores were isolated as described above, and the spore concentration was analyzed using a hemocytometer.

2.6. Extraction and analyses of endogenous plant steroids

Steroid extraction was performed using 20 mg lyophilized plant material as described in Shiko et al. (2023). In brief: Flash-frozen plant material was lyophilized. The dried material was pulverized, and 20 mg aliquots of each sample were extracted with 1 mL of extraction mixture (80% MeOH in water containing 100 ng mL^{-1} progesterone-d_9 as internal standard, Merck, Germany). Samples were vortexed for 60 s and sonicated (Sonorex Super RK 100 H, BANDELIN electronic, Germany) for 5 min at 22 °C. The crude extracts were centrifuged (HERMLE ZK233-M2, HERMLE Labortechnik GmbH, Germany) for 60 s at 16,000 *g*, and the supernatant used for the Steroid analysis. It was performed by LC-MS/MS on an Agilent 1260 series HPLC system (Agilent Technologies) with a tandem mass spectrometer QTRAP 6500 (SCIEX, Darmstadt, Germany). A detailed description of the method and the results are presented in the supplement (Suppl. Table S1, Suppl. Table S2, and Suppl. Table S3).

2.7. Phytosterol analysis

The analysis by gas chromatography single quadrupole MS (GC-MS) was performed on a 7820A Agilent gas chromatograph coupled to a MSD 5977B single quadrupole and 7693A autosampler with a split/splitless injector. Instrument control and data analysis were carried out with Agilent MassHunter Workstation Software package B.08.00 (Santa Clara, CA, USA). An Agilent HP-5MS UI capillary column of 30 m, 0.25mm inner diameter, 0.25 μm film thickness was used at a constant flow rate of 1.4 mL min^{-1}. Carrier gas was helium 99.999% from Linde AG (Munich, Germany). The single quadrupole (MS) was operated with electron ionization (EI) at 70 eV. The multiplier operated with a gain factor of 5. The samples were analyzed using a scan method (*m/z* 100–600). The total run time of the method was 20.0 min. The initial column temperature was 60 °C and was held for 1.0 min. Then the temperature was ramped up to 260 °C with 50 °C min^{-1}. The steroids were eluted at a rate of 5 °C min^{-1} until 310 °C. At the end, the temperature was increased to 320 °C at a rate of 50 °C min^{-1} (hold time 2.4

min). The solvent delay was 8.5 min. The injection volume was 3 μL. The injection was performed in a splitless mode at an injector temperature of 250 °C. The temperature for the MS transfer line was set at 250 °C, for the MS source at 230 °C, and for the MS quadrupole at 150 °C. The sterols were identified by mass spectral analysis and by calculating the relative retention time in comparison with commercial references (a detailed description of the method can be found in the supplement (Suppl. Table S4).

The sample preparation procedure started with the comminution of the samples to ensure a homogeneous material. Approximately 5 mg of each sample was weighed and transferred into a 20 mL glass vial. The concentration was then adjusted to 1 mg mL^{-1} by adding 2 M aqueous NaOH solution, followed by incubation at 80 °C for 2 h. After incubation, the sample was homogenized by vortexing to ensure uniformity. The sample preparation procedure is described in detail by Müller et al., (2017). Briefly, 1000 μL aliquot was taken from the sample and 100 μL of internal standard mix (1 μg mL^{-1} desmosterol-d_6 and 1 μg mL^{-1} cholesterol-d_7 in ethyl acetate) was added. 650 μL of *tert*-butyl methyl ether (TBME) was added and the mixture was homogenized by hand for 1 min. Afterwards, the sample was centrifuged for 5 min at 11,000 g. The organic phase was transferred to a second microcentrifuge tube containing a mixture of 40 mg of anhydrous magnesium sulfate and PSA (7:1; dispersive solid-phase extraction(dSPE)). The extraction was repeated with an additional 750 μL of TBME. The organic phases from both extractions were combined into the dSPE mixture, homogenized again and centrifuged for 5 min at 11,000 g. The supernatant was transferred to a GC-Vial and the solvent was evaporated under a gentle stream of nitrogen until the sample was dry. Finally, the sample underwent derivatization according to the method described by Junker et al., (2021) for the analysis of oxysterols. The detailed results are given in the supplement (Suppl. Table S5).

2.8. Phytohormone extraction and analyses

Plants were treated with 3 and 10 μM DHEA. Therefore, 60 μL of a 2.5 mM or an 8.34 mM DHEA stock solution (dissolved in DMSO) were added to 50 mL tap water, while 60 μL DMSO in 50 mL tap water (=0.12% DMSO) was used as mock-treatment. *A. thaliana* or *H. vulgare* shoots, or *S. polyrhiza* plants were harvested 0.5, 1, and 3 h after the start of the treatment and immediately frozen in liquid nitrogen. 100–250 mg of the frozen plant material was homogenized using mortal and pistil in liquid nitrogen. Samples were extracted in 1 mL methanol containing 40 ng salicylic acid-d_4 (Santa Cruz Biotechnology, TX, USA), 40 ng jasmonate-d_6 (HPC Standards GmbH, Germany), 40 ng abscisic acid-d_6 (Toronto Research Chemicals, Toronto, Canada), and 8 ng jasmonate-isoleucin-d_6 (HPC Standards GmbH, Cunnersdorf, Germany) as internal standards. Phytohormone analysis was performed by liquid chromatography (LC)-mass spectrometry (MS)/MS as described in Heyer et al. (2018) on an Agilent 1260 series HPLC system (Agilent Technologies, Santa Clara, CA, USA) with the modification that a tandem mass spectrometer QTRAP 6500 (SCIEX, Darmstadt, Germany) was used. A more detailed phytohormone analysis is presented in the supplement (Suppl. Table S6).

2.9. RNAseq analysis

7 days old *A. thaliana* plants were transferred to PNM medium. After 2 days of adaption to the new medium, plants were treated with 10 μM DHEA (dissolved in 0.12% DMSO), while 0.12% DMSO was used as a mock-treatment. Shoots were harvested after 1 h and immediately frozen in liquid nitrogen. Additionally, *A. thaliana* plants were infected with *A. brassicicola* spore solution (in 0.12% DMSO) or spore solution supplemented with 10 μM DHEA (in 0.12% DMSO). Shoots were harvested after 24 h and immediately frozen in liquid nitrogen. All samples were stored at −80 °C. RNA was isolated using TRIzol® Reagent (Invitrogen™ by Thermo Fisher Scientific, MA, USA), as described previously (Chomczynski, 1993; Shiko et al., 2023). Integrity and concentration of plant RNA were analyzed using absorbance analysis with a NanoVue (GE Healthcare, Uppsala, Sweden).

Four biological replicates of all treatments and controls were analyzed by GENEWIZ Germany GmbH (Azenta Life Science, Leipzig, Germany) and processed as described in the following:

RNA samples were quantified using Qubit 2.0 Fluorometer (Life Technologies, Carlsbad, CA, USA) and RNA integrity was checked using Agilent Fragment Analyzer (Agilent Technologies, Palo Alto, CA, USA). RNA sequencing library preparation was prepared using NEBNext Ultra II RNA Library Prep Kit for Illumina following manufacturer's instructions (NEB, Ipswich, MA, USA). Briefly, mRNAs were first enriched with Oligo(dT) beads. Enriched mRNAs were fragmented. First strand and second strand cDNA were subsequently synthesized. The second strand of cDNA was marked by incorporating dUTP during the synthesis. cDNA fragments were adenylated at 3′ends, and indexed adapter was ligated to cDNA fragments. Limited cycle PCR was used for library amplification. The dUTP incorporated into the cDNA of the second strand enabled its specific degradation to maintain strand specificity. Sequencing libraries were validated using NGS Kit on the Agilent Fragment Analyzer (Agilent Technologies, Palo Alto, CA, USA), and quantified by using the Qubit 4.0 Fluorometer (Invitrogen, Carlsbad, CA, USA). The sequencing libraries were multiplexed and loaded on the flow cell on the Illumina NovaSeq 6000 instrument according to manufacturer's instructions. The samples were sequenced using a 2 × 150 Pair-End (PE) configuration v1.5. Image analysis and base calling were conducted by the NovaSeq Control Software v1.7 on the NovaSeq instrument. Raw sequence data (.bcl files) generated from Illumina NovaSeq was converted into fastq files and de-multiplexed using Illumina bcl2fastq program version 2.20. One mismatch was allowed for index sequence identification. Raw data are available on ncbi (Geo accession ID: GSE261582).

Raw sequencing reads were assessed for quality using FastQC (version 0.11.9; https://www.bioinformatics.babraham.ac.uk/projects/fastqc). Adaptor trimming, quality filtering, and read preprocessing were performed using fastp (version 0.23.2; Chen et al., 2018). In detail, 5′ and 3′ bases with a Phred quality score below 28 were cut, and reads were removed if they had more than one ambiguous base, an average quality score below 28, or a length of fewer than 15 bases. Processed reads were aligned to the current *A. thaliana* genome (tair10.1) using Hisat2 (version 2.2.1) with standard parameters (Kim et al., 2019). The aligned reads were sorted and indexed using SAMtools (version 1.11; Li et al., 2009). Read counting was performed using featureCounts (version 2.0.1; Liao et al., 2014) with the tair 10.1 annotation as reference. Differential gene expression analysis was performed using DESeq2 (version 1.38.3; Love et al., 2014), and comparisons having a false discovery rate (FDR; Benjamini and Hochberg, 1995) adjusted p value < 0.05 were deemed to be statistically significant.

Genes were categorized according to their function found on The Arabidopsis Information Resource (TAIR) database (February 2024) (Berardini et al., 2004). Keywords for each gene with locus identifier numbers were selected from GO-term classifications using an original code utilizing python and pandas library (McKinney, 2010). The code provided matches for the locus number with functions (GO-terms) recorded on TAIR, the number of genes that a function has matched with, as well as a bubble plot with desired variables from the RNAseq results.

2.10. Quantitative polymerase chain reaction

To verify the reliability of the RNAseq experiment, we quantified the expression PR1 by quantitative polymerase chain reaction (qPCR). qPCRs were executed as described previously (Klein et al., 2021a,b; Shiko et al., 2023). In brief: RNA was transcribed into cDNA by a RevertAid First Strand cDNA Synthesis Kit (ThermoFisher Scientific, Waltham, MA, USA). qPCRs were performed in a Bio-Rad CFX96

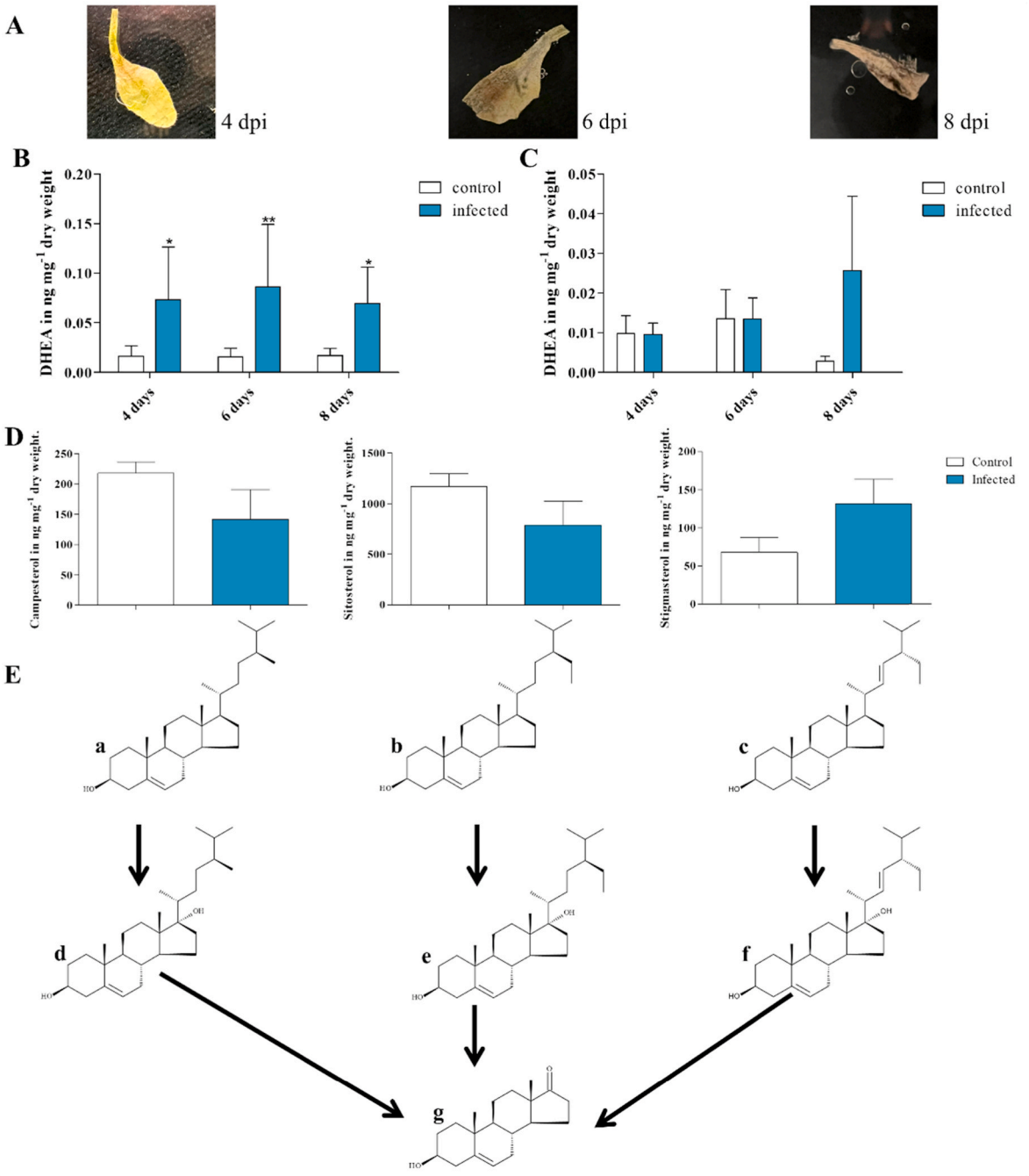

Fig. 2. Putative pathway leading to enhanced dehydroepiandrosterone (DHEA) accumulation in *A. brassicicola*-infected *A. thaliana* plants. (**A**) We here show leaves of *A. thaliana* 4, 6 and 8 days post infection (dpi) with *A. brassicicola*. (**B**) The graph shows DHEA values (blue) compared to the control (white) 4, 6, and 8 days post-infection (dpi). DHEA concentrations are given in ng mg^{-1} dry weight (means ± SEM are shown; $n > 3$; $p < 0.05$). An asterisk indicates significant differences. (**C**) We give here additionally the DHEA values of *A. thaliana* roots of plants with *A. brassicicola*-infected shoots. The graph shows DHEA values (blue) compared to the control (white) 4, 6, and 8 days post-infection (dpi). DHEA concentrations are given in ng mg^{-1} dry weight (means ± SEM are shown; $n > 3$; $p < 0.05$). No statistically significant differences could be detected. (**D**) Moreover, we show the contents of campesterol, sitosterol, and stigmasterol in *A. brassicicola*-infected *A. thaliana* shoots 4 dpi compared to uninfected controls. Sterol concentrations are given in ng mg^{-1} dry weight (means ± SEM are shown; $n > 3$; $p < 0.05$). No statistically significant differences could be detected. (**E**) In mammals, DHEA is produced from pregnenolone with 17α-hydroxypregnenolone as intermediate. For plants, a direct conversion of sterols into DHEA was discussed (Shiko et al., 2023). In contrast to mammals, phytosterol precursors are more abundant compared to cholesterol. Therefore, a possible scenario for plants could be that the formation of DHEA starts from campesterol (**a**), β-sitosterol (**b**), or stigmasterol (**c**). A 17α-hydroxylation leads to the formation of the intermediates 17α-hydroxycampesterol (**d**), 17α-hydroxy-β-sitosterol (**e**), or 17α-hydroxystigmasterol (**f**). DHEA (**g**) could be formed by 17,20-lyase reactions of these 17α-hydroxysterols. (For interpretation of the references to color in this figure legend, the reader is referred to the Web version of this article.)

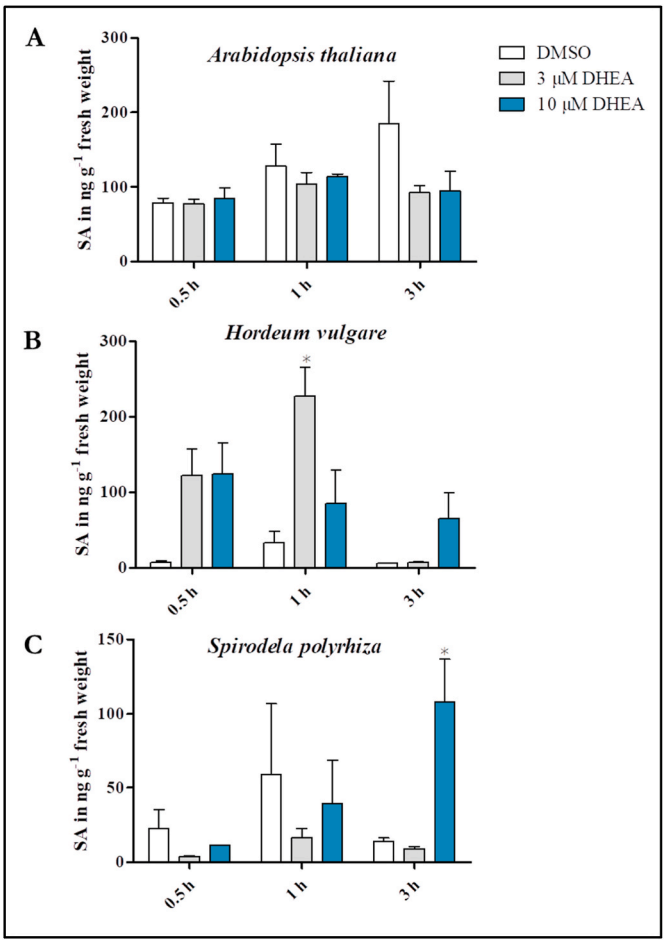

Fig. 3. Effects of exogenously applied DHEA on salicylic acid in plants. *A. thaliana* (**A**) and *H. vulgare* (**B**) were germinated and cultivated in long-day conditions for 7 days. *S. polyrhiza* clones (**C**) were cultivated for 7 days in sugar-free medium according to Appenroth et al. (1996). Plants were treated with DHEA (3 or 10 µM) solutions. DMSO (0.12% in water) was used as a mock-treatment. Plant material (shoots of *A. thaliana* and *H. vulgare* and complete *S. polyrhiza* plants) was harvested after 0.5, 1, and 3 h. Hormones were extracted from fresh shoot material. The graph depicts the salicylic acids (SA) concentrations in ng g^{-1} fresh weight (Mean ± SEM are shown; $4 \leq n \geq 3$). Differences were analyzed statistically by a one-way ANOVA with post hoc Bonferroni correction ($p < 0.05$).

Thermal Cycler (Bio-Rad Laboratories Inc., Göttingen, Germany). For each measurement a 20 µL reaction was prepared with 1.1 µL cDNA, 2 dNTPs (10 mM; ThermoFisher Scientific, Waltham, MA, USA), 1 µL EvaGreen® Plus Dye (Biotium, USA), 2 µL of each primer (100 µM), 0.2 µL DreamTaq DNA Polymerase, and 3.4 µL DreamTaq DNA Polymerase buffer (ThermoFisher Scientific, Waltham, MA, USA) were used. qPCRs were performed with a preincubation at 95 °C for 180 s, followed by 40 cycles at 95 °C for 10 s, 60 °C for 50 s, and 72 °C for 60 s. The following primers for qPCRs were used:

JK_ RPS18_for: 5′GTCTCCAATGCCCTTGACAT'3
JK_ RPS18_rev: 5′ TCTTTCCTCTGCGACCAGTT'3
JK_AtPR1_for: 5′TCAGTGAGACTCGGATGTGC'3
JK_AtPR1_rev: 5′CGTTCACATAATTCCCACGAG'3

Four biological replicates were analyzed. We compared the normalized Count Reads of PR1 obtained by RNAseq and the CT values of PR1 obtained by qPCR, as well as the calculated Log2 fold changes (RNAseq) and relative expression (qPCR). Relative expression was calculated by $2^{-\Delta\Delta CT}$ method (Livak and Schmittgen, 2001). RPS18 was used as reference gene for normalization as described before (Shiko et al., 2023).

2.11. Aequorin luminescence-based assay of intracellular calcium

The measurement of intracellular calcium follows the protocol described by Vadassery et al. (2009). *A. thaliana* lines expressing a cytosolic apoaequorin from *Aequorea victoria* (based on ecotype RLD) were used for Ca^{2+} measurements (Polisensky and Braam, 1996). Plants were grown vertically in Hoagland's medium with 1% agar for 16 days. Roots were dissected from shoots and both reconstituted in 5 µm coelenterazine solution (P.J.K. GmbH, Kleinblittersdorf, Germany) containing 30 µM DHEA, DMSO (mock treatment) or water as control in the dark overnight at 21 °C. Bioluminescence counts (BIC) in *Arabidopsis* from roots were recorded as relative light units (RLU) sec^{-1} in 5 s intervals for 20 min using a microplate luminometer (Luminoscan Ascent, version 2.4, Thermo Fisher Scientific, Waltham, USA). After a 1-min background reading, H_2O_2 (Carl Roth GmbH, Karlsruhe, Germany) was added manually to the well (final concentration: 40 mM) and readings in RLU were taken for 20 min. Calibrations were performed by estimating the amount of aequorin remaining at the end of experiment by discharging all remaining aequorin in 0.1 M $CaCl_2$, 10% ethanol, and the counts were recorded for 10 min. The luminescence counts obtained were calibrated using the equation by Rentel and Knight (2004) that takes a double logarithmic relationship between the concentration of free Ca^{2+} present in the cell and the remaining aequorin discharged at any point of time into account. The calibration equation is: $pCa = 0.332588(-\log \boldsymbol{k}) + 5.5593$, where $\boldsymbol{k}$ is a rate constant equal to luminescence counts sec^{-1} divided by total remaining counts. Results are given in the supplement (Suppl. Table S7).

2.12. Determination of the ergosterol biosynthesis pattern by GC-MS

To understand the ergosterol biosynthesis pathway in *A. brassicicola*, we analyzed the sterol pattern of azole-treated *A. brassicicola* hyphae. Therefore, we determined a non-lethal concentration of ketoconazole (KC; Merck, Darmstadt, Germany). We infected PDS plates supplemented with 0.5, 1, 2, 4, and 8 µg mL^{-1} KC, using PDA supplemented with methanol (0.1%) as mock-treatment. Sterol pattern were analyzed in *A. brassicicola* hyphae grown for 7 days in potato dextrose broth (PDB; pH = 6.5–6.8; Carl Roth GmbH, Germany) supplemented with 2 µg mL^{-1} KC, while methanol was used as mock-treatment. As a control, potato-dextrose agar supplemented with methanol (solvent for KC; 1) was used. Influence of DHEA on production of ergosterol in *A. brassicicola* was tested using PDB supplemented with 10 µM DHEA dissolved in DMSO, while pure DMSO was used as mock-treatment. Fungal tissue was harvested by centrifugation (10 min, 12,000 *g*, 22 °C) and lyophilized for 24 h.

Fungal tissue was harvested by centrifuging and lyophilized for 24 h. To determine the effect of DHEA treatment on the ergosterol biosynthesis pathway, the samples were analyzed by gas chromatography (GC) coupled to quadrupole MS. For analysis 2 × 5 mg lyophilized fungal biomass were used. The isoprenoid and the sterol pattern were determined by previously described protocols (Müller et al., 2017; Liebl et al., 2023). A detailed description of the analysis of isoprenoid and ergosterol patterns is found in the supplement (Suppl. Table S8). Content and composition of intermediates of the isoprenoid and post-lanosterol pathway of ergosterol biosynthesis of *A. brassicicola* samples confronted with 10 µM DHEA or ketoconazole compared to untreated controls can be found in the supplement (Suppl. Table S9).

2.13. Rhodamine-based membrane integrity assay

A plug of well-grown *A. brassicicola* mycelium (d = 5 mm) was cultivated in 3 mL PDB for 72 h. DHEA (30 µM; solved in DMSO) or DMSO (0.12 %; as mock-treatment) were added and the fungus was cultivated for additional 24 h. Rhodamine B (Merck, Darmstadt, Germany) dissolved in ethanol was added to a final concentration of 50 µM. After 30 min incubation the fungal tissues were washed in tap water.

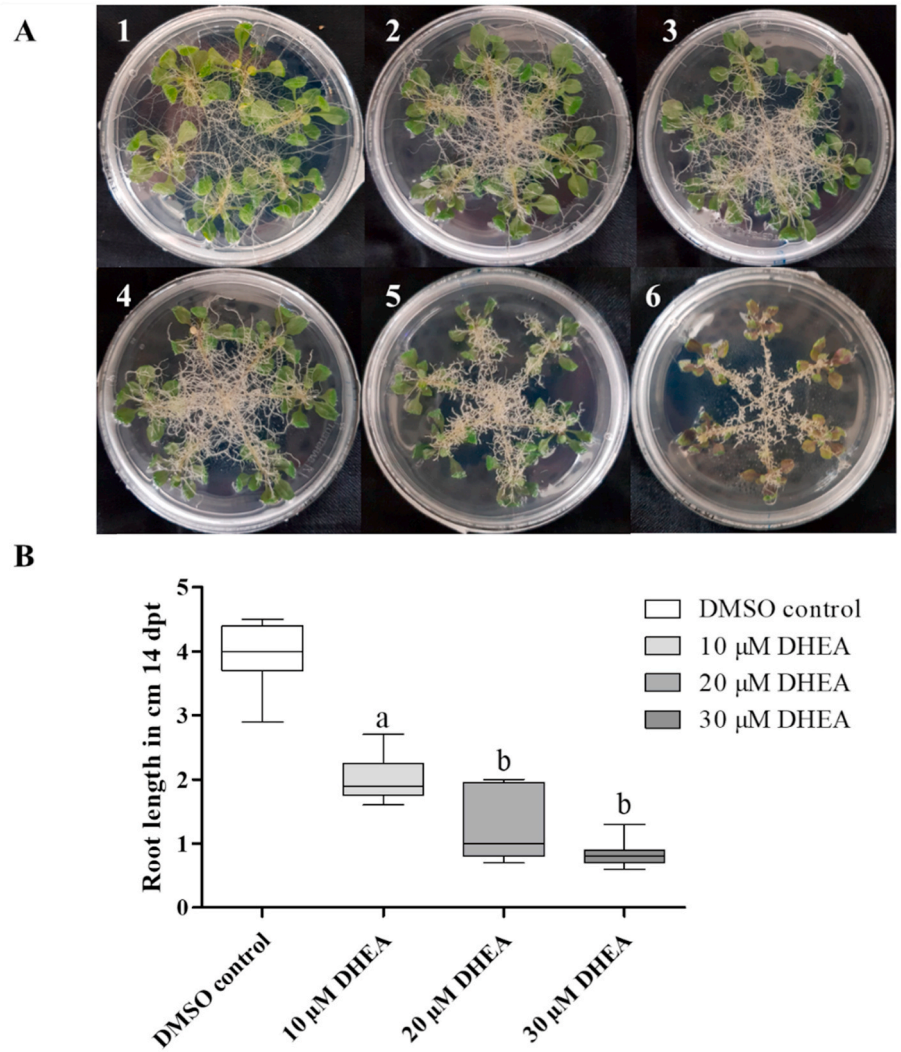

Fig. 4. Effects of exogenous DHEA on root growth and morphology. (**A**) *A. thaliana* plants were germinated on MS and cultivated in long-day conditions. 10-day old plants were transferred on MS-medium containing DHEA (3–30 μM dissolved in 0.12% DMSO). The graph shows pictures of plant roots 14 days after the treatment (days post-treatment dpt; DMSO (1), 3 μM DHEA (2); 5 μM DHEA (3); 10 μM DHEA (4); 20 μM DHEA (5); 30 μM DHEA (6). (**B**) Root length of 14 days old plants directly sown on DHEA-containing medium. Differences were analyzed statistically by a one-way ANOVA with post hoc Bonferroni correction (Mean ± SEM are shown; $10 \leq n \geq 8$; $p < 0.05$).

2.14. Statistical analysis

All data are expressed as the means ± SEM. Values of biological replicates are given as n within the **Figure** legends. Means between the various groups were compared by *t*-Test or one-way analysis of variance (ANOVA followed by Tukey's post hoc test). In case of multiple comparisons, a post hoc Bonferroni correction was applied. P values < 0.05 were considered statistically significant. Data were analyzed using GraphPad Prism 5 Software (GraphPad).

3. Results and discussion

3.1. DHEA levels and DHEA formation in A. brassicicola infected plants

It has been shown previously that exogenous treatment with progestogens helps plants cope with moderate (a)biotic stress (Genisel et al., 2013; Janeczko et al., 2013; Hao et al., 2019; Sabzmeydani et al., 2020; reviewed in: Klein, 2024). Therefore, we analyzed changes in *A. thaliana*'s endogenous progestogens and the chemically related androgens after infection with the economically critical pathogenic fungi *A. brassicicola*. We show that infection of *A. thaliana* leaves with *A. brassicicola* enhances the amounts of DHEA in the shoot material by factor 5 (Fig. 2B). Pregnenolone and progesterone could be detected only in shoots of infected plants, while the 17α-hydroxypregnenolone, 17α-hydroxyprogesterone, androstenedione, testosterone, 5α-dihydroprogesterone were not detected at all (shoots: Suppl. Table S2; roots: Suppl. Table S3). Additionally, we detected changes in the 5α-pregnane-3,20-dione levels of roots (Suppl. Table S3), but data and changes were not consistent. That is why we focuses on the detected elevated DHEA levels. Changes in the DHEA profiles could not be detected in the roots of these plants after 4, and 6 days of infection (Fig. 2C). Only 8 days post infection (dpi), we were able to detect enhanced DHEA values, but these changes were not statistically significant. We conclude that infection of *A. thaliana* shoots with the fungal pathogen *A. brassicicola* enhances the DHEA level in the infected tissue. We suggest that the enhanced values of DHEA after 8 dpi are caused by transport of DHEA or by growth of the phytopathogen into the roots.

Since we could not detect DHEA in *A. brassicicola* spores and hyphae when the fungus was cultivated on PDA medium, the elevated DHEA levels in infected *A. thaliana* shoots could be of plant origin or originating from a fungal precursor. We have shown previously that the aquatic monocot *Spirodela polyrhiza* does not contain endogenous DHEA,

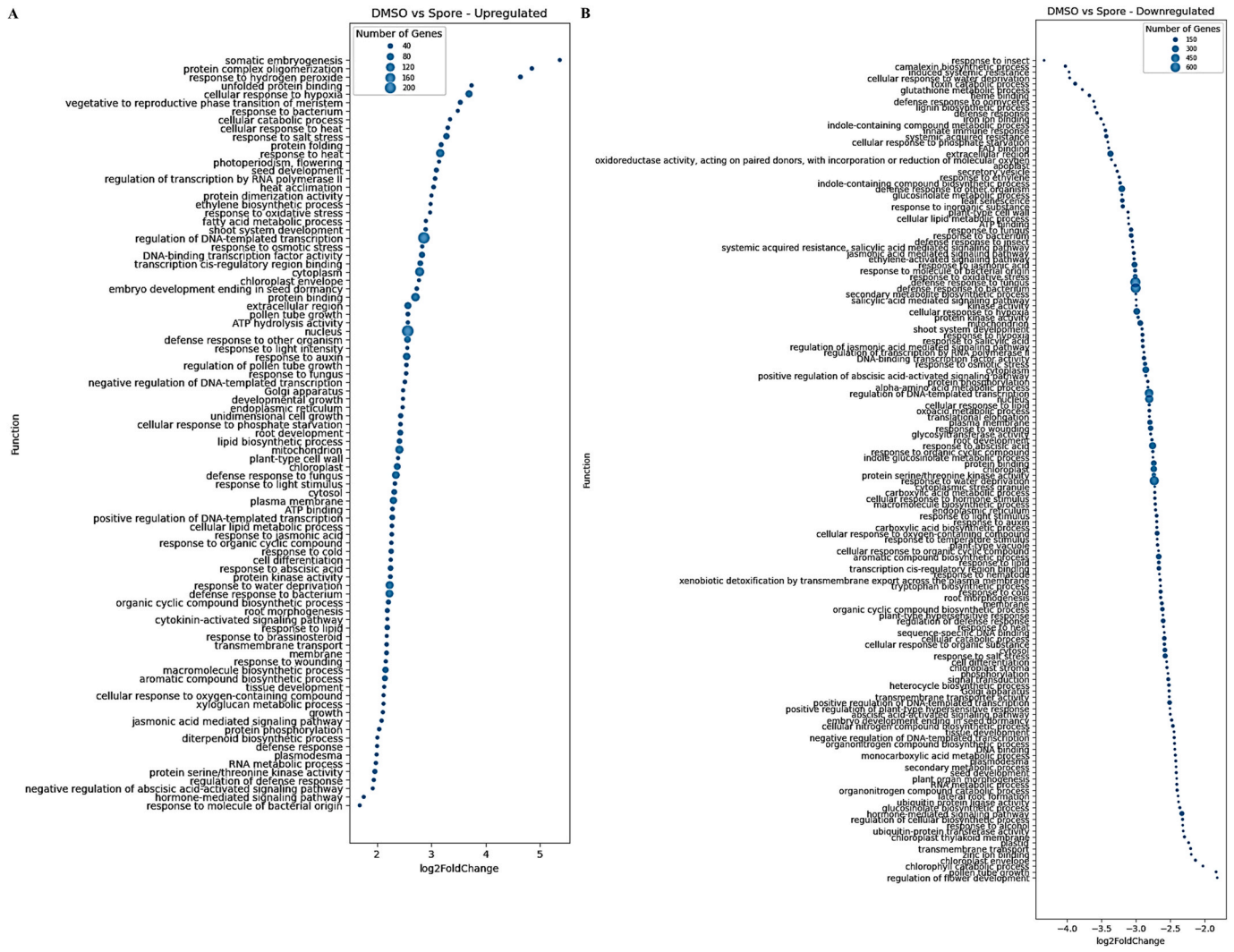

Fig. 5. Effects of *A. brassicicola* infection on gene expression of *A. thaliana*. The graph summarizes genes changed by DHEA treatment. The function-association of significantly changed transcripts ($p < 0.05$) is based on TAIR database. The graph shows the number of changed transcripts associated with a particular function.

but converts steroid precursors quite efficiently into DHEA (Shiko et al., 2023). Since *A. brassicicola* can also infect *S. polyrhiza* leaves (Suppl. Fig. S1), we tested whether DHEA accumulates in *S. polyrhiza*, because the host plant converts a fungal precursor to DHEA. In previous studies we did not find DHEA in *S. polyrhiza*, but the plant was able to catalyze the conversion of progestogens into androgens (Shiko et al., 2023). Therefore, *S. polyrhiza* is able to convert the fungal precursor into DHEA (Shiko et al., 2023). We have to mention that we found small amounts of DHEA slightly above the detection limit in uninfected *S. polyrhiza* within these experiments. Nevertheless, DHEA values did not increase upon *A. brassicicola* infection.

We conclude that fungal precursors do not cause enhanced DHEA values in the infected *S. polyrhiza* host. If we assume that this is also true for *A. thaliana*, the elevated DHEA levels in the *A. brassicicola* – infected shoots could be caused by an altered steroid metabolism which leads to the observed enhanced DHEA levels in the infected plant organ. A possible scenario could be that the pathogen alters the phytosterol metabolism in *A. thaliana*. While the direct conversion of sterols into C_{19}-steroids is not known for mammalians (pregnenolone is the precursor of all mammal steroids), a conversion of phytosterols and ergosterol was detected in Mycobacteria (Dovbnya et al., 2010). A comparable conversion of phytosterols could lead to the detected elevated DHEA levels in *Arabidopsis* shoots. In line with this theory, we could show that *A. brassicicola*-infected *A. thaliana* plants showed changed sterol profiles compared to uninfected controls 4 days post infection (Suppl. Table S5). While the contents of squalene and cholesterol did not change in infected A. thaliana shoots, we found slightly reduced values of campesterol and sitosterol, while the values of stigmasterol were slightly increased. On a systematic level, it can be mentioned that no cholesterol was found in uninfected *A. thaliana* roots, while we were able to identify it in 2 of 3 experiments using infected root material. This indicates a changed sterol metabolism, which could lead to an enhanced DHEA production. This nicely fits to a metabolomics analysis of infected *A. thaliana* plants by Botanga and colleagues (Botanga et al., 2012), which could show that cholesterol levels of *A. thaliana* plants are significantly reduced 9 and 24 h after infection with *A. brassicicola*. A putative way from the three changed phytosterols in infected shoots (campesterol, sitosterol and stigmasterol) to DHEA is depicted in Fig. 2E. These possible pathways of DHEA formation have to be analyzed in further experiments.

3.2. Effects of DHEA treatment on plants

We could show that DHEA was enhanced in *A. thaliana* shoots infected with *A. brassicicola*, while this was not the case for *S. polyrhiza*. Therefore, we analyzed the effects of exogenously applied DHEA on these two plant species, while using DMSO as an organic solvent. Organic solvents are causing stress in plant cells. As a result SA

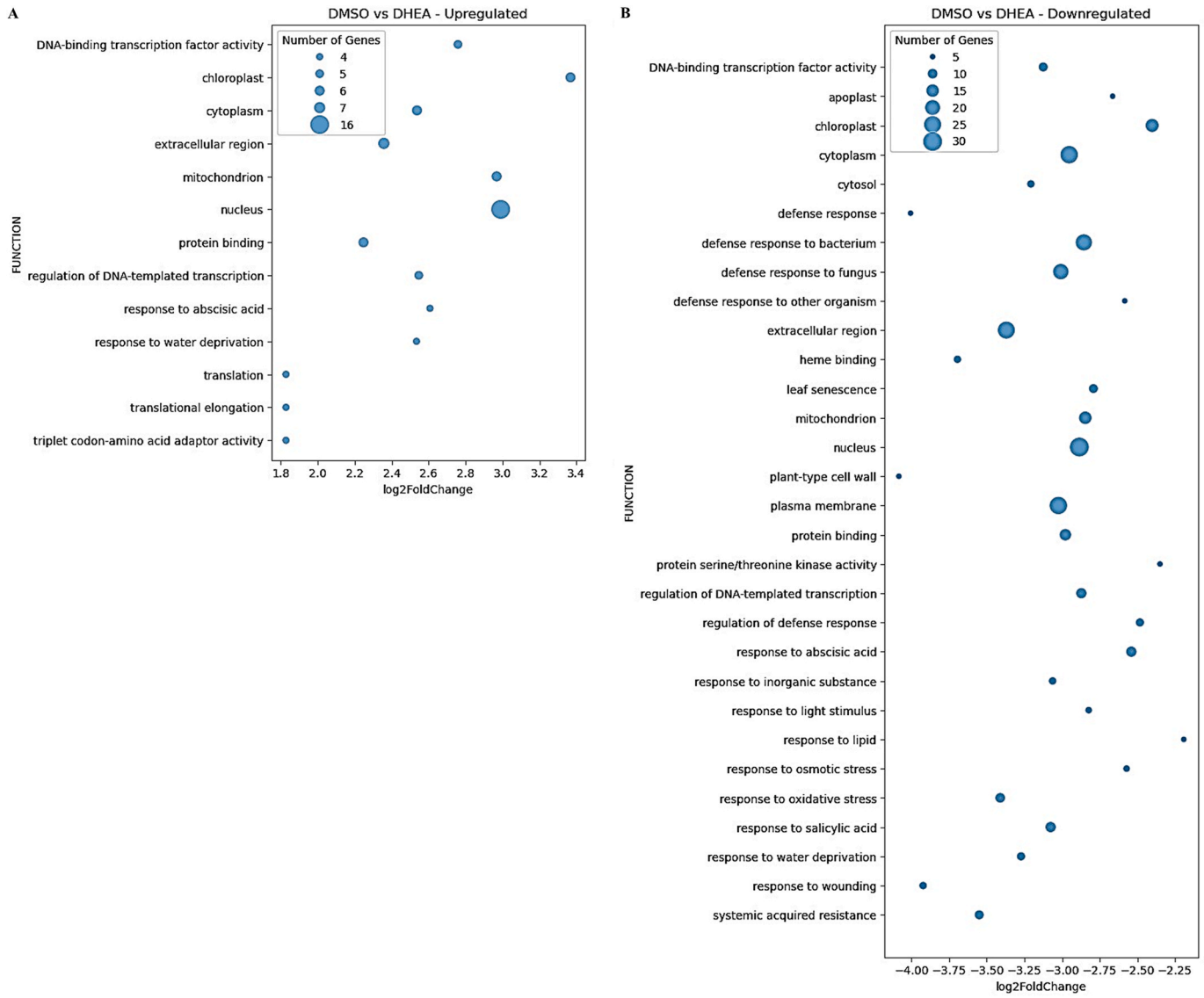

Fig. 6. Effects of DHEA on gene expression of *A. thaliana* 1 h after treatment. The graph summarizes genes changed by DHEA treatment. The function-association of significantly changed transcripts ($p < 0.05$) is based on TAIR database. The graph shows the number of changed transcripts associated with a particular function.

accumulates in DMSO treated plants. While we have a peak in *S. polyrhiza* after 3 h, there is a constant, but not statistically significant increase in *A. thaliana*. An increase in SA could not be seen in DHEA treated *Arabidopsis* shoots, while DHEA-treated S. polyrhiza plants accumulated DHEA with a peak 3 h of treatment for *S. polyrhiza*. (Fig. 3).

To determine if SA accumulation as response to DHEA-treatment is *S. polyrhiza*-specific, we analyzed the effects of DHEA on another monocot species (*H. vulgare*), too. We were able to detect a SA accumulation in this species, too. In contrast to *S. polyrhiza* we found a SA peak for *H. vulgare* after 1 h. In summary, the reaction of both monocot species to DHEA is quite complicated and no direct dose-dependency can be detected. We conclude that DHEA activates SA-dependent pathogen response in both analyzed monocot species, but at least at the observed time points, not in *A. thaliana*. If there is a general difference in the effects of DHEA on monocots and dicots must be shown in further experiments.

We could detect effect even in other stress related phytohormones for the analyzed plant species. For *A. thaliana* 10 μM DHEA lead to peaks of jasmonate and its conjugate jasmonoyl isoleucine (JA-Ile) (Suppl. Fig. S2), In *H. vulgare* 3 μM DHEA lead to a peak of cis-OPDA levels (a bioactive JA precursor). Treating this monocot species with 10 μM DHEA results in reduced cis-OPDA levels, while a carboxylated JA (COOH-JA) peak was detected (Suppl. Fig. S3). In *S. polyrhiza* 10 μM DHEA lead to elevated JA levels and a reduction of hydroxylated JA-Ile conjugates (OH-Ja-Ile; Suppl. Fig. S4). We conclude that DHEA leads to changes of stress hormone reaction for all analyzed plant species.

Moreover, we recognized a strong effect of DHEA-supplemented MS-medium on the root growth of *A. thaliana* (Fig. 4). Root growth was significantly reduced dose-dependently when 10 μM DHEA or higher concentrations were found in MS-medium. For 20 and 30 μM DHEA, reduced shoot growth and the formation of anthocyanins could be detected. It is unclear if this is caused by DHEA transport into the shoot material or starvation of the shoot material caused by limited root development. Additionally, 3 μM DHEA lead to slightly thicker roots, but the effect was not statistically significant.

To get first insights into the mode of action of DHEA in plants, we realized an RNAseq experiment. 9-days-old *A. thaliana* plants on PNM were infected with *A. brassicicola* and harvest after 24 h (Fig. 5), or treated for 1 h with DHEA (in 0.12% DMSO), while 0.12% DMSO was used as a mock-treatment (Fig. 6). Moreover, 9-day-old *A. thaliana*

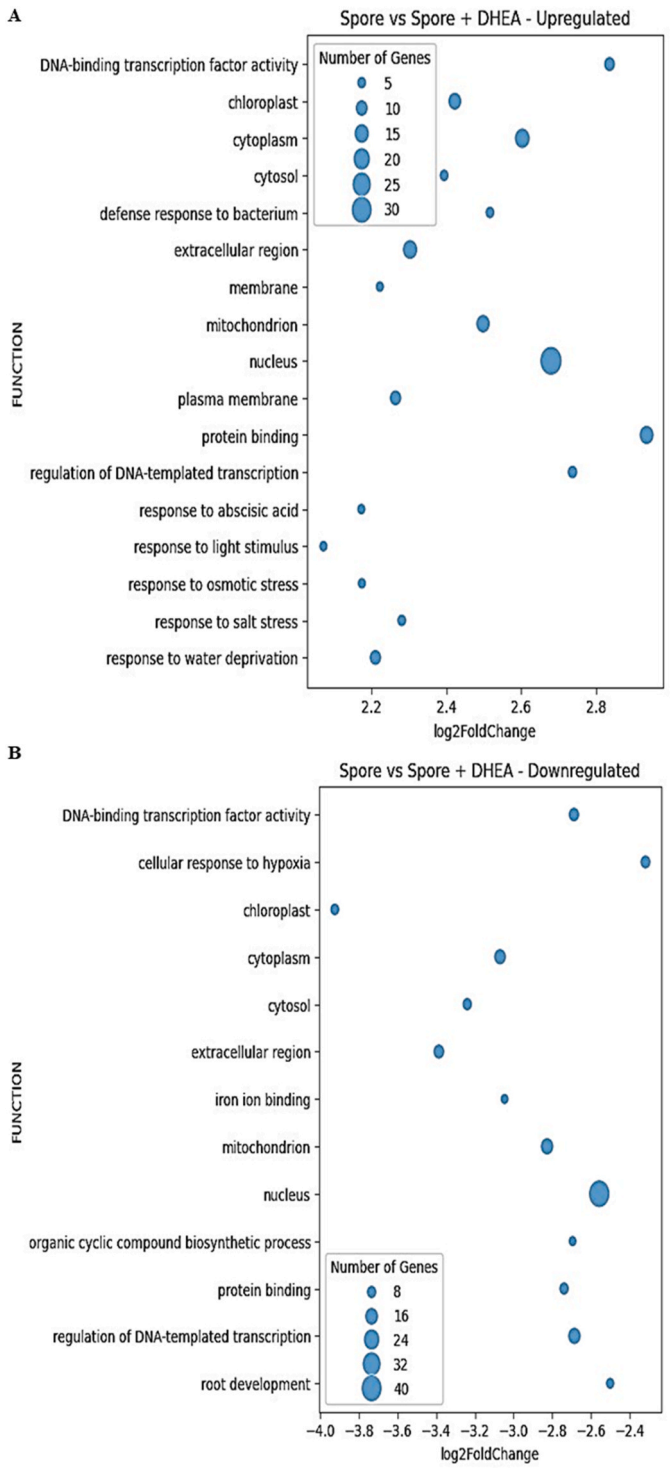

Fig. 7. Effects of DHEA on gene expression of infected *A. thaliana* plants one day post infection. The graph summarizes genes changed by infection with DHEA-supplemented *A. brassicicola* spores compared to a non-treated infection. The function-association of significantly changed transcripts ($p < 0.05$) is based on TAIR database. The graph shows the number of changed transcripts associated with a particular function.

plants were infected with an *A. brassicicola* spore solution (spores in 0.12% DMSO) or a spore solution supplemented with 10 μM DHEA. Shoots of infected plants were harvested 24 h after infection and immediately shock-frozen (Fig. 7).

To ensure the trustworthiness of our RNAseq data, we compared the normalized Count Reads of PR1 obtained by RNAseq and the CT values of PR1 obtained by qPCR, as well as the calculated Log2 fold changes (RNAseq) and relative expression (qPCR). Results can be found in the supplement (Table S5).

As assumed, infected and non-infected plants showed the biggest difference (DEGs can be found in Suppl. Table 10). 24 h after infection led to significant ($p < 0.05$) upregulation of 777 genes (log_2FoldChange >1.5) and downregulation of 1677 genes (log_2FoldChange < -1.5; Fig. 5). (MA plots can be found in the supplement; Suppl. Fig. S5). This includes an upregulation of genes regulating abiotic stress responses. *A. brassicicola* is a necrotrophic fungus. It is not surprising that *A. brassicicola* infection induces primarily jasmonic acid induced responses (jasmonic acid mediated signaling pathway is not inducing programmed cell death), while elements of the SA mediated signaling are downregulated (SA-mediated systemic acquired resistance leads to programmed cell death). It was described previously, that JA drives defense response against *Alternaria* (exemplarily in apple leaves; Zhang et al., 2023). The suppression of certain parts of the stress response can be explained by the mutual exclusivity of the JA and SA signaling pathways (Caarls et al., 2015; Le Phuong et al., 2020), or by the restriction of specific defense responses (e.g., camalexin biosynthesis; Schuhegger et al., 2007) to the site of infection. Additionally, the activity of *A. brassicicola* effectors may interfere with the expression of defense-related genes as it was shown for other phytopathogenic ascomycota (see here exemplarily for *Ustilaginoidea virens*-infections of rice; Fan et al., 2019).

Moreover, we could detect changes of transcripts of the plant metabolism. This includes many loci associated with oxidative stress, which is indicating the typical oxidative-burst of the fungal infection (Kámán-Tóth et al., 2019). Additionally, reprogramming of phenylpropanoid biosynthetic pathway involving lignin, hydroxycinnamic acids, scopoletin, anthocyanin genes was detected in *A. thaliana* after infection with *Alternaria brassicae* (Hamsa et al., 2024). Together with our data this indicates a strong change of the plant metabolism in response to infection.

Compared to *A. brassicicola*-infection DHEA-treatment results only in small differences within the *A. thaliana* transcriptome. Nevertheless, 1 h DHEA treatment led to significant ($p < 0.05$) upregulation of 62 genes (log_2FoldChange >1.5) and downregulation of 137 genes (log_2FoldChange < -1.5; Fig. 6). Infection of *A. thaliana* with a DHEA-containing spore solution led to the significant upregulation of 30 genes, while 35 genes were downregulated compared to mock infection (Fig. 7). Many of the downregulated genes are either directly or indirectly involved in defense and immune responses (58 of the 137 genes are described in TAIR to be involved in (a)biotic stress responses), code for channels or transporters (6 genes), enzymes required for cell wall synthesis or modifications (5 genes), control root (hair) growth (5 genes), repressors of growth and development (3 genes), auxin metabolism and GH3-mediated auxin conjugation (5 genes), enzymes involved in secondary defense metabolite biosynthesis (10 genes), redox regulation (8 genes), Ca^{2+} signaling and ubiquitination (2 genes each). This suggests that exogenously applied DHEA represses defense and stress responses as well as root (hair) growth. This could explain the detected changes of DHEA-treated *A. thaliana* roots. Genes which are upregulated by DHEA promote translation and amino acid metabolism (7 genes), transcription (5 genes), developmental processes including flower development (3 genes), lipid metabolism (2 genes), growth *via* auxin and gibberelin functions (2 genes), ubiquitination (3 genes), maintain cellular homeosstasis and prevent cell death (1 gene). Therefore, up-regulated genes predominantly involved in processes promoting development and cellular functions. We therefore presume that exogenous DHEA shifts the balance between the antagonistic principles of stress response and growth towards growth. Moreover, we observed that a high percentage of DHEA-regulated genes were located in cell membranes (24% of the upregulated and 35% of the downregulated genes). A complete list of differential gene expression (DGE) between DHEA-treated and mock-treated *A. thaliana* shoots can be found in the supplement (Suppl.

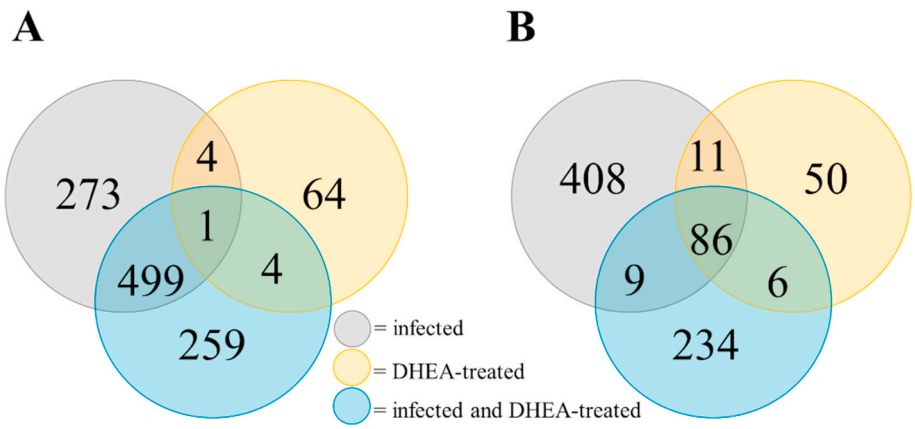

Fig. 8. Transcriptome changes by infection, DHEA-treatment, and both. We here show a Venn diagram that shows the numbers of genes differently expressed by infection, DHEA-treatment, and both infection and DHEA-treatment. We could show that all this conditions lead to a strong change of the transcriptomes. While the upregulated genes are comparable different (only one gene shared by all 3 conditions), a bigger set of shared genes is downregulated (78).

Table S11). Also infected plants treated with DHEA showed a strong change of membrane-associated genes (24% of the upregulated and 34% of the downregulated genes are localized in membranes). Interestingly, both treatments lead only to a minimal change of proteins annotated as cytosolic protein. A complete DGE list of transcripts differing between infected and infected and DHEA-treated *A. thaliana* shoots can be found in the supplement (Suppl. Table S12).

It was demonstrated previously that DHEA enhanced the permeability of mitochondria in human TM-3 cells (Shen et al., 2012; Liu et al., 2016). This could explain the changed mRNA values of membrane-localized proteins and the enhanced expression of genes associated with water deprivation detected in both plants treated with DHEA and infected + DHEA-treated (Fig. 6; Fig. 7).

Comparing the transcriptomes of plants infected with a DHEA-containing spore solution to uninfected control (MA plot can be found in Suppl. Fig. 5C) leads to the following results: 24 h infection led to significant ($p < 0.05$) upregulation of 763 genes (log2FoldChange >1.5) and downregulation of 1498 genes (log2FoldChange < −1.5; Fig. 5). If we compare genes infected plants and plants infected with DHEA-containing spore solution (MA plot can be found in Suppl. Fig. 5D), we can see that many genes which were transcribed in an enhanced manner (Fig. 7A) were somehow defense associated (defense response to bacteria, response to abscisic acid, response to osmotic stress, response to salt stress and response to water deprivation) and associated with changes in the membrane (membrane and plasma membrane). Portions are comparable to those found for DHEA-treated plants compared to the mock-treated control. Moreover, a lot of genes associated with cell organelles were changed (chloroplast, cytoplasm, cytosol, mitochondrion, nucleus). Considering that all organelles are cell compartments built by membranes, we see this as additional hint that DHEA changes membrane characteristics. It must be mentioned that even a lot of organelle-associated genes were downregulated (Fig. 7B).

All in all, we could detect that all 3 tested conditions (infected, DHEA-treated, and infected + DHEA-treated) lead to partially comparable changes of the *A. thaliana* transcriptome. It was analyzed which amount of the transcriptional changes was shared by all conditions. A Venn diagram can be found in Fig. 8. Nearly no common pattern could be identified in the upregulated genes. Only transcripts of locus At2g21910 were found at elevated levels in all conditions (Suppl. Table S13). At2g21910 encodes the P450-enzyme CYP96A5. P450 enzymes are monooxygenases many of them are involved in steroid metabolism (exemplarily: human CYP11A1; Schiffer et al., 2016; human CYP17A1; Neunzig et al., 2014; plant CYP87A4; Carroll et al., 2023). Considering that all conditions show higher DHEA concentrations, compared to the control, it can be discussed if CYP96A5 is involved in the steroid metabolism of *A. thaliana*. Unfortunately, the enzymatic machinery of steroid metabolism in plants is poorly understood. Nevertheless, a protein blast against animalia (https://blast.ncbi.nlm.nih.gov/Blast.cgi?PROGRAM=blastp&PAGE_TYPE=BlastSearch&LINK_LOC=blasthome [December 18, 2024]) shows the ultra-long-chain fatty acid omega-hydroxylase-like of *Ostrea edulis* and *Mercenaria*, as well as the cholesterol 24-hydroxylase-like of *Poecilia latipinna*, *Poecilia formosa*, *Scleropages formosus*, *Poeciliopsis prolifica*, within the first results. Nevertheless, the hypothesis that CYP96A5 is involved in plant steroid metabolism has to be challenged in further experiments.

More common genes can be found that are downregulated (Fig. 8). From the 86 genes found downregulated (Suppl. Table S13) in all conditions around 10% are associated with the regulation of the defense response (At1g14880, At1g19250, At1g33960, At2g14560, At3g57260, At4g12500, At5g40990, At5g44420, At5g45090, At5g64810). Additionally, nearly 10% of the DEGs are involved in regulating oxygen-dependent reactions (At1g53620, At1g60740, At1g60750, At1g69880, At3g28580, At4g15330). We explain this with membrane disturbances caused by fungal infection or DHEA. In line with this hypothesis, around 10% of all genes downregulated in all conditions are membrane-/transport-associated (At1g12940, At1g21245, At1g74080, At2g29350, At3g28510, At5g41390).

Based on RNAseq experiments, we built the hypothesis that DHEA disturbs the integrity of plasma membranes in *A. thaliana* and *A. brassicicola*. This hypothesis is supported by the fact, that 12 plasma membrane-associated genes were downregulated in DHEA-treated *A. thaliana* shoots. It has to be mentioned, that we can't rule out that DHEA affects other membranes of plant cells, too. To analyze the effects of DHEA on membrane-integrity of *A. thaliana*, we treated roots of a transgenic *A. thaliana* line expressing the cytosolic apoaequorin from *A. victoria* (Polisensky and Braam, 1996) in 30 μM DHEA using DMSO as mock treatment. After 24 h we used an aequorin-based assay to analyze the intracellular Ca^{2+} accumulation in response to hydrogen peroxide treatment. We expected that reduced membrane integrity will induce at least partial, membrane depolarization. This should lead to disturbed Ca^{2+} elevation into the cytosol. In line with this hypothesis we could detect significantly reduced Ca^{2+} peaks in *A. thaliana* roots pre-treated with DHEA compared to the mock-treatment (Fig. 9). A strong difference was also seen for DHEA-treated shoots compared to the water control, but this difference was also detected in DMSO controls. Nevertheless, we see these results as additional proof of reliability of RNAseq data.

Enhanced membrane-permeability could also explain the observed changes in ABA and SA regulated genes (Fig. 6), while no changes in SA and ABA concentrations were detectable in *A. thaliana* (Fig. 5). ABA and SA are transported in protonated form to their target, where they will be

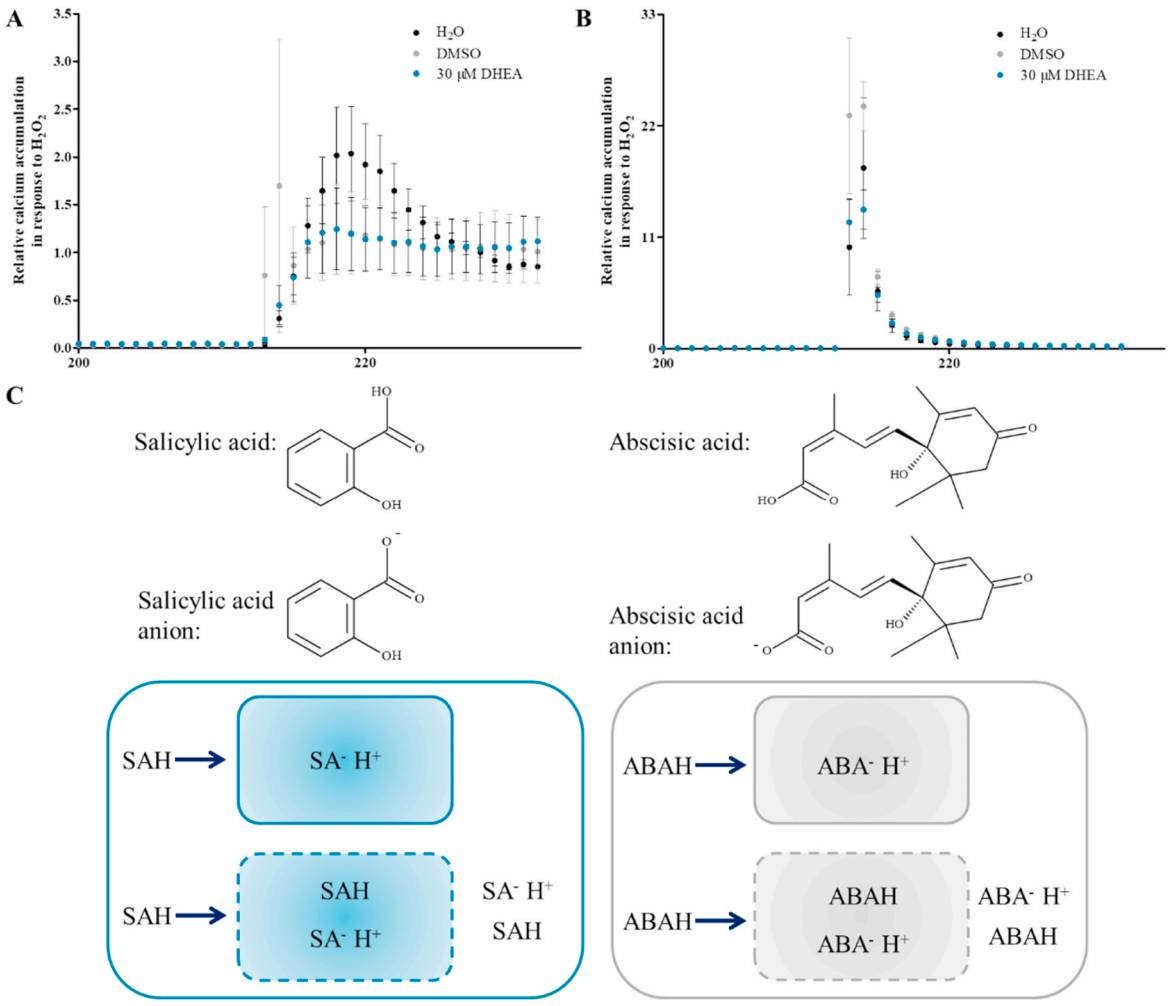

Fig. 9. Calcium-accumulation in *A. thaliana* roots pretreated with DHEA in response to H_2O_2. Shoots (**A**) and roots (**B**) of *A. thaliana* were pretreated with 30 µM DHEA while H_2O and DMSO were used as mock-treatments. Bioluminescence counts (BIC) in *Arabidopsis* from roots were recorded as RLU sec^{-1} in 5 s intervals for 20 min using a microplate luminometer. After a 1-min background reading, 40 mM H_2O_2 as added manually to the well and readings in RLU were taken for 20 min. The graph depicts the luminescence peak measured 16.83 min after the treatment. All data are given as mean ± SEM (n control = 6; n DHEA = 8). The difference between the peak values was analyzed using a *t*-test; indicating a statistically significant difference for Ca^{2+} accumulation in the roots ($p = 0.0057$), but no statistically difference between DMSO and DHEA in the shoot. (**C**) Abscisic and salicylic acid are transported in protonated forms to their targets. As weak acids, both hormones can diffuse bio-membranes passively. The pH values of the cytosol will lead to conversion into anionic forms of both phytohormones. Anionic forms of abscisic and salicylic acid cannot cross plasma membranes. This results in the expression of abscisic and salicylic acid-regulated genes. In cases of enhanced membrane permeability, deprotonated forms of salicylic and abscisic acid could leave the cytosol, which results in reduced expression of abscisic or salicylic acid-regulated genes.

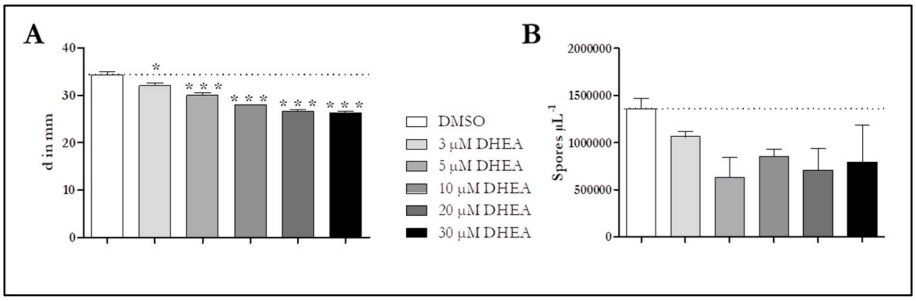

Fig. 10. Effects of DHEA on *A. brassicicola*. A plug of well-grown *A. brassicicola* tissue (diameter = 5 mm; a) or a solution of *A. brassicicola* spores was transferred to PDA medium containing different concentrations of DHEA or DMSO as control. The size of the *A. brassicicola* colony (**A**) or the number of spores produced by these colonies (**B**) were analyzed after 7 days. The graph depicts mean ± SEM. Differences were analyzed statistically by a one-way ANOVA with post hoc Bonferroni correction (*$p < 0.05$; ***$p < 0.001$; n = 3).

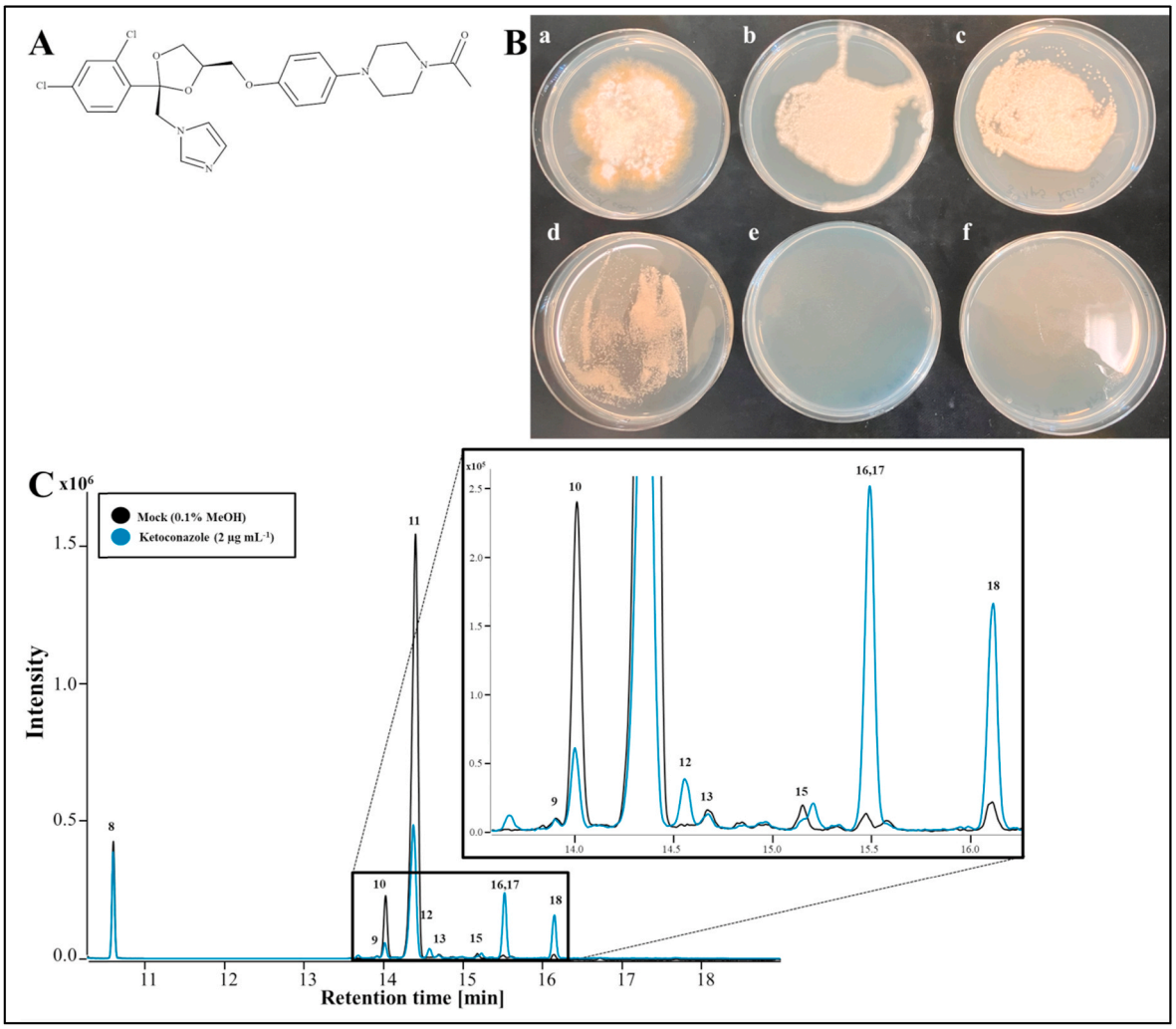

Fig. 11. Ketoconazole treatment of *Alternaria brassicicola*. To determine non-lethal concentrations of ketoconazole (KC; **A**) for *Alternaria brassicicola*, a spore solution was spread on potato-dextrose agar (**B**) supplemented with methanol (0.1%; solvent of KC; **a**) or 0.5 (**b**), 1 (**c**); 2 (**d**); 4 (**e**), and 8 (f) µg mL^{-1} KC dissolved in methanol. Plates were photographed 72 h after infection. The lethal concentration was found to be between 2 and 4 µg mL^{-1} KC. (**C**) GC-MS was used to determine ergosterol biosynthesis pattern. The figure depicts the representative selected ion chromatograms (*m/z* 217 + 251+343 + 363+393 + 407 + 466 + 467 + 469) of detected intermediates of untreated *A. brassicicola* sample (black) and sample confronted with 2 µg mL^{-1} KC (turquois) after 7 days; internal standard = cholestane (**8**), ergosta-5,8,22,24(28)-tetraen-3β-ol (**9**), lichesterol (ergosta-5,8,22-trien-3β-ol, **10**), ergosterol (ergosta-5,7,22-trien-3β-ol, **11**), 14-methylfecosterol (14-methylergosta-8,24(28)-dien-3β-ol, **12**), ergosta-5,7,22,24(28)-tetraen-3β-ol (**13**), episterol (ergosta-7,24(28)-dien-3β-ol, **15**), 14-methylergosta-8,24(28)-dien-3β,6α-diol (**16**), lanosterol (4,4,14-trimethylcholesta-8,24-dien-3β-ol, **17**), eburicol (4,4,14-trimethylergosta-8,24(28)-dien-3β-ol, **18**).

deprotonated. Anions of ABA and SA cannot cross plasma membranes. Consequently, ABA and SA accumulate in their target cells, where they induce the expression of SA- or ABA-related genes (Rocher et al., 2006; Rocher et al., 2009). In DHEA-treated plants, the intercellular transport mechanism of ABA and SA is strongly disturbed, and anions of SA and ABA can also leave the cytosol, which results in reduced expression of ABA or SA inducible genes. Moreover, enhanced bio-membrane permeability hampers the maintenance of the pH value needed for ABA and SA deprotonation In summary, this leads to a disfunctional intercellular transport of ABA and SA, resulting in decreased expression of SA or ABA related genes without reduced SA levels in the plant matrix. Moreover, this membrane disturbance can also explain why DHEA-treated *A. thaliana* shoots show lower SA levels after 3 h of treatment compared to the mock-treated control (Fig. 3A).

3.3. Effects of DHEA on A. brassicicola

Considering that elevated DHEA values were detected in response to fungal infections in infected *A. thaliana* shoots (Fig. 2B), we asked the question: Has DHEA an effect on fungal pathogens?

We used the economically relevant *A. brassicicola* as our model system to analyze this question. Cvelbar and colleagues (Cvelbar et al., 2013) showed that DHEA has the most substantial growth-inhibiting effects of all tested progestogens and androgens on the analyzed ascomycetous fungi (*Hortaea werneckii*, *Saccharomyces cerevisiae,* and *Aspergillus oryzae*) followed by the androgens testosterone and androstenedione. Therefore, we analyzed if DHEA treatment can reduce the growth and spore production of *A. brassicicola* (Fig. 10).

We could show that DHEA reduces the growth and spore production of *A. brassicicola* in a dose-dependent manner (Fig. 10). This could be seen already for 3 µM DHEA. In contrast to changes in growth rates, changes in spore production are not statistically significant.

Cvelbar and colleagues (Cvelbar et al., 2013) assumed that reduced growth of ascomycetous fungi is caused by disturbed ergosterol biosynthesis. Ergosterol is the major sterol of fungal cell membranes (Zinser et al., 1993; Suchodolski et al., 2019) of nearly all fungi (Weete et al., 2010). Moreover, ergosterol is a transitory cell wall component, on its way to the extracellular environment, or it plays a role, for

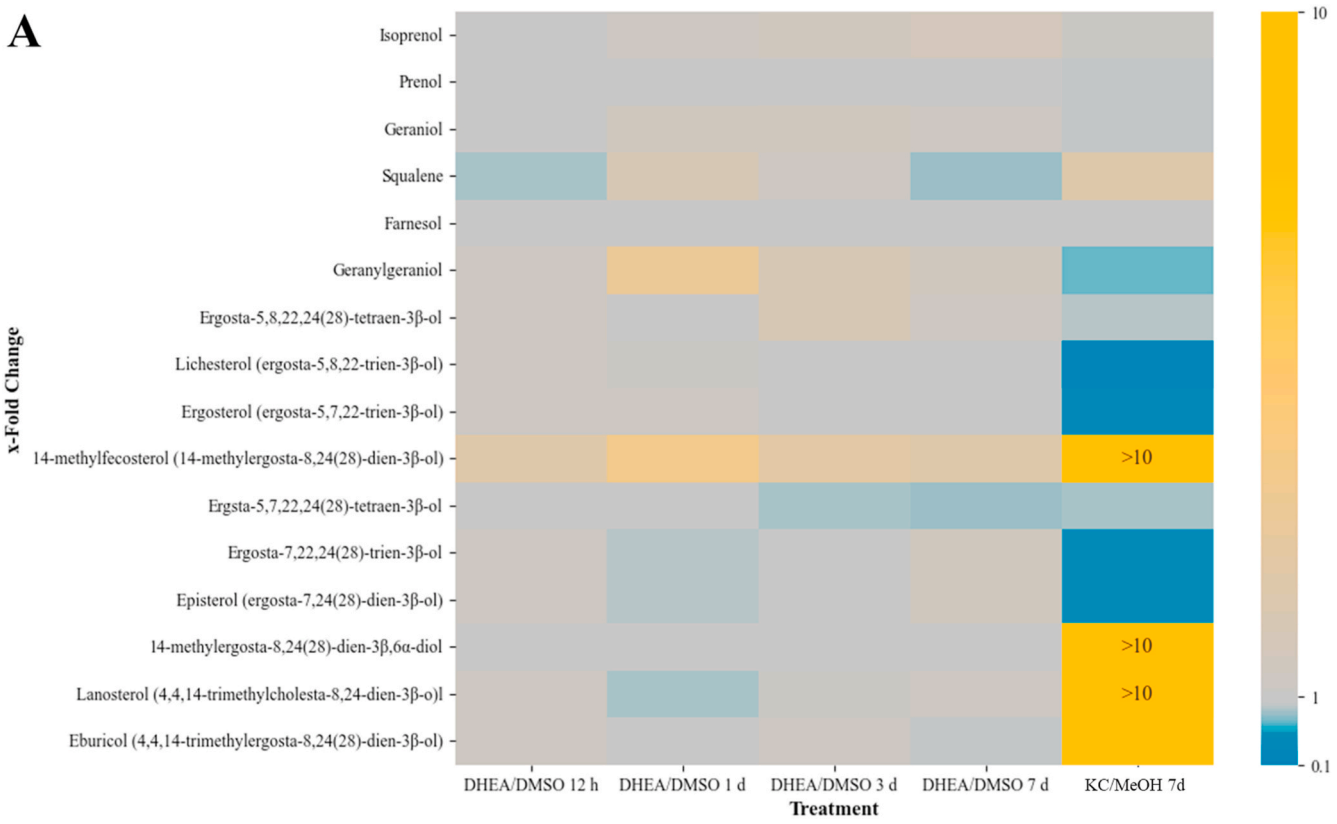

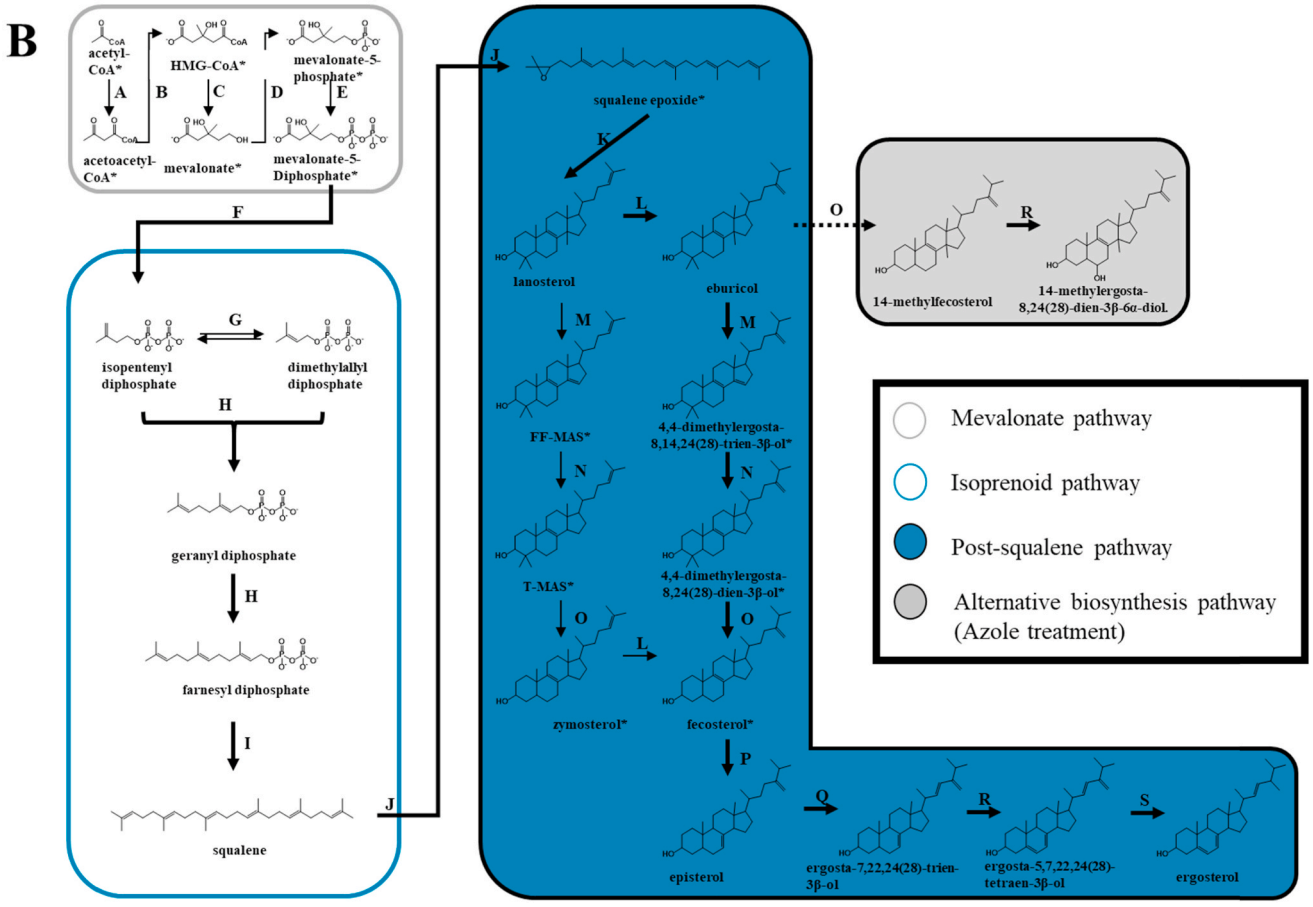

(caption on next page)

Fig. 12. Heatmap of intermediates of the isoprenoid and post-lanosterol pathway of ergosterol biosynthesis of *A. brassicicola* samples confronted with dehydroepiandrosterone (10 μM; DHEA) or ketoconazole (2 μg mL^{-1}; KC) compared to mock-treated controls (DMSO or MeOH) and the identified favored ergosterol pathway of *A. brassicicola*. **(A)** Isoprenoid pyrophosphates were analyzed by GC-MS as their corresponding isoprenoid *tert*-butyldiphenylsilyl ether by GC-MS after enzymatic pyrophosphate cleavage to the free isoprenoid and subsequent derivatization with tert-butyldiphenylchlorosilane. The relative amount has been normalized to untreated samples (Gsaller et al., 2016; Krauβ et al., 2021). Boxes in yellow color >10-fold changes, in grey color no changes were observed (change = 1), and in blue color <0.1-fold changes. (**B**) Here we show the putative ergosterol biosynthesis pathway of *A. brassiciola*.; this schematic ergosterol biosynthesis covers not all detected intermediates from the table in the supplement (Table S09); **Metabolites:** acetyl-coenzyme A, acetoacetyl-coenzyme A, β-hydroxy β-methylglutaryl-coenzyme A (HMG-CoA), mevalonate, mevalonate-5-phosphate, mevalonate-5-diphosphate, isopentenyl diphosphate, dimethylallyl diphosphate, geranyl diphosphate, farnesyl diphosphate, squalene, squalene epoxide, lanosterol (4,4,14-trimethylcholesta-8,24-dien-3β-ol), eburicol (4,4,14-trimethylergosta-8,24(28)-dien-3β-ol), FF-MAS (4,4-dimethylcholesta-8,14,24-trien-3β-ol), 4,4-dimetylergosta-8,14,24(28)-trien-3β-ol, T-MAS (4,4-dimethylcholesta-8,24-dien-3β-ol, 4,4-dimethylergosta-8,24(28)-dien-3β-ol, zymosterol (cholesta-8,24-dien-3β-ol), fecosterol (ergosta-8,24(28)-dien-3β-ol), episterol (ergosta-7,24(28)-dien-3β-ol), ergosta-7,22,24(28)-trien-3β-ol, ergosta-5,7,22,24(28)-tetraen-3β-ol, ergosterol (ergosta-5,7,22-trien-3β-ol), 14-methylfecosterol (14-methyl-ergosta-8,24(28)-dien-3β-ol), 14-methylergosta-8,24(28)-dien-3β,6α-diol ; **Enzymes:** acetyl-coenzyme A-acetyltransferase (ACAT, **A**), β-hydroxy β-methylglutaryl-coenzyme A synthase (HMG-CoA synthase, **B**), β-hydroxy β-methylglutaryl-coenzyme A reductase (HMG-CoA reductase, **C**), mevalonate kinase (**D**), phosphomevalonate kinase (**E**), diphosphomevalonate decarboxylase (**F**), isopentenyl diphosphate isomerase (**G**), farnesyl diphosphate synthase (**H**), squalene synthase (**I**), squalene epoxidase (**J**), oxidosqualene cyclase (OSC, **K**), sterol C24-methyltransferase (24-SMT, **L**), sterol C14-demethylase (**M**), sterol C14-reductase (N), sterol C4-demethylase complex (**O**), sterol C8-isomerase (**P**), sterol C22-desaturase (**Q**), sterol C5-desaturase (**R**), sterol C24-reductase (**S**). * not detected intermediates or not part of the analysis (mevalonate pathway). (For interpretation of the references to color in this figure legend, the reader is referred to the Web version of this article.)

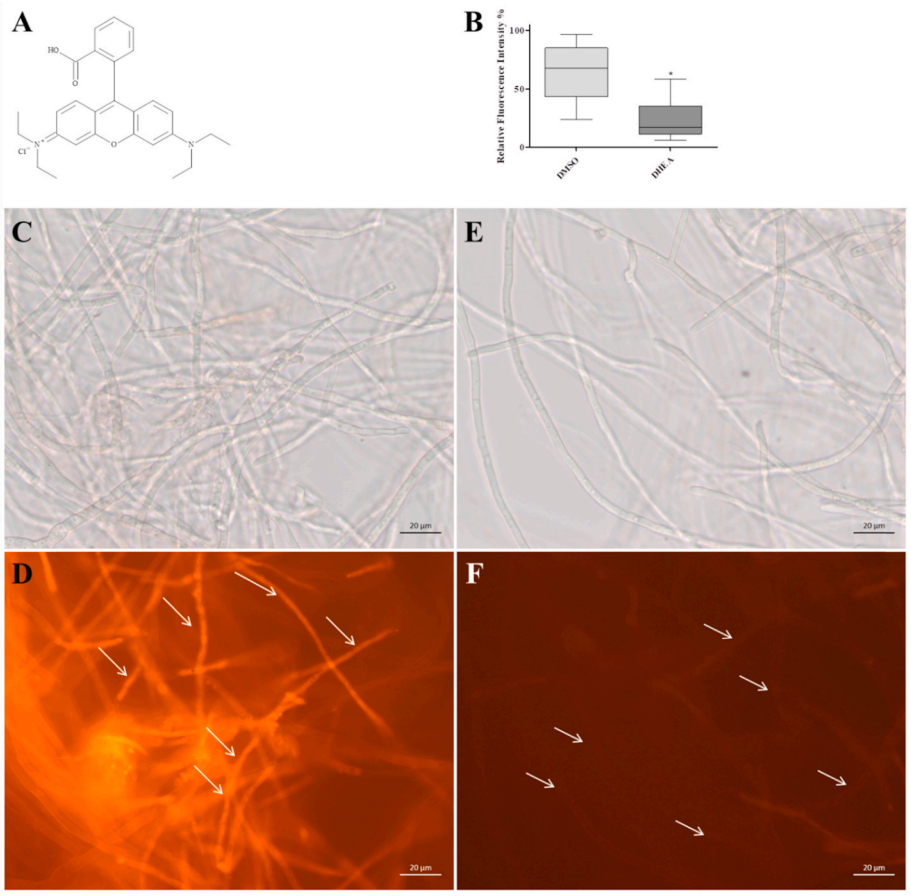

Fig. 13. Rhodamine B-based assay for membrane integrity of *A. brassicicola*. Rhodamine B (**A**) is a fluorescence dye was used to detect depolarization and de-energization of mitochondria pretreated with 30 μM DHEA or mock-treated with DMSO for 24 h. Relative fluorescence intensity (RFI) was calculated using the highest fluorescence value of each experiment as reference (in all cases a value of the DMSO-treated control). The results are given as mean ± SEM (n = 78; statistical analysis with *t*-Test; $P < 0.001$). Microscopic inspections of mock-treated hyphae (C and D) and DHEA-treated hyphae (E and F) are depicted. For comparism bright-field images (C and E) are shown as well as fluorescence images by the use of DsRED filter (D and F). High fluorescence (D) or no fluorescent hyphae (F) are indicated by white arrows.

instance, in the formation of cell wall carbohydrate patches. Particularly, eburicol seems to play a prominent role in this latter process (Geiβel et al., 2018; Elsaman et al., 2024). That is why the mode of action of many commercially available fungicides (e.g., KC used in the treatment of fungal infections of human cutis or mucus; Poojary, 2017; or fungicides used in agriculture e.g., chiral triazole fungicides like prothioconazole; Zhang et al., 2019) is inhibition of ergosterol biosynthesis (Müller et al., 2013; reviewed in: Campoy and Adrio, 2017).

Ergosterol can be produced in an eburicol-dependent or an eburicol-independent pathway (Hosseini et al., 2024). These pathways differ in the preferred substrate of the involved sterol C14-demethylase (lanosterol or eburicol). Fungal sterol C14-demethylases can be inhibited by

azole fungicides (e.g., KC; Venkateswarlu and Kelly, 1996). We analyzed which concentration of KC is lethal for *A. brassicicola* (Fig. 11B). We determined the preferred pathway of ergosterol biosynthesis in *A. brassicicola* to analyze the effects of DHEA on ergosterol biosynthesis. This was done by analyzing ergosterol pattern of *A.brassicicola* in presence of KC compared to mock-treated controls, as shown before (Müller et al., 2018).

Therefore, the highest non-lethal concentration of KC (2 μg mL^{-1} in our experiments) was used to treat *A. brassicicola* for 7 days. These tissues (hyphae and spores) of *A. brassicicola* were used to analyze sterol patterns.

We could show that eburicol accumulates after KC treatment by factor 9 (50 ng mg^{-1} in the control and 450 ng mg^{-1} in KC treatment; Fig. 11), while lanosterol is enhanced by factor 10 (25 ng mg^{-1} in the control and 280 ng mg^{-1} in KC treatment; Fig. 11). Therefore, we assume that the sterol C14-demethylase of *A. brassicicola* is not very substrate-specific but a substrate-promiscous enzyme. Keeping in mind that lanosterol is a precursor of eburicol in eburicol-dependent ergosterol biosynthesis, we assume that the eburicol-dependent ergosterol pathway is preferred in *A. brassicicola*. A predicted pathway for ergosterol biosynthesis in *A. brassicicola* can be found in Fig. 12. The determined sterol pattern of *A. brassicicola* can be used to analyze next-level fungicides against the agricultural important *Alternaria* species.

A. brassiciola were cultivated in liquid PDA for 0.5 d (12 h), 1 d, 3 d, and 7 d confronted with 10 μM DHEA, while 0.12% DMSO was used as mock-treatment. We analyzed patterns of the mevalonate pathway, the isoprenoid pathway, and the post-squalene pathway (Fig. 12). We were not able to detect a reduction of ergosterol in the DHEA-treated fungus compared to the control, but interestingly 14-methylfecosterol accumulated by factor 3 in the DHEA-treated fungus for all analyzed time point. In contrast KC treated *A. brassiciola* showed 90 times higher concentrations of 14-methylfecosterol. Additionally, we could detect an increase of squalene by factor 2, as well as the accumulation of 14-methylergosta-8,24(28)-dien-3β,6α-diol (from levels under detection limit to 360 ng mg^{-1} dry weight), lanosterol (factor 10), and eburicol (factor 9). In contrast lichesterol (factor 5), ergosterol (factor 5), ergosta-7,22,24(28)-trien-3β-ol (factor 2), and episterol (factor 2) were found reduced. The highest reduction total (4000 ng mg^{-1}) was detected for ergosterol in KC treated fungal cells. KC-treatment leads to eburicol accumulation in *A. brassicicola*. This indicates that ergosterol biosynthesis favors the eburicol-dependent pathway in this fungus. Nevertheless, based on these results we suggest that DHEA inhibits the growth of the ascomycetous fungus *A. brassicicola* in an ergosterol-independent way if this is the case for other ascomycetous plant-pathogens (e.g., *Verticillium dahliae*) has to be determined in future experiments.

Fungi and Mammalia are both part of the Opisthokonta group of the eukaryotes. Therefore, the biomembranes of fungi and mammalia are highly similar (Ntow-Boahene et al., 2023). Keeping in mind that DHEA causes enhanced membrane-permeability in human cells (Shen et al., 2012; Liu et al., 2016), we hypothesize that enhanced membrane-leakage can cause the reduced growth of *A. brassicicola* confronted with DHEA. We assume that this is an adaption of the plant metabolism to fungal attack that helps plants fight fungal pathogens.

To get first data ensuring this hypothesis, we performed Rhodamine B staining of *A. brassicicola* liquid cultures treated for 24 h with 30 μM DHEA or control. We observed that Rhodamine B fluorescence of DHEA pretreated hyphae is just 35% of the mock-treated control (Fig. 13). This can be caused by depolarization and de-energization of mitochondria and impaired mitochondrial function, indicating a loss of mitochondria membrane integrity (Brilhante et al., 2018). Therefore, we assume that membrane-changes are the working principle causing the reduced growth of DHEA-treated *A. brassicicola* hyphae.

Keeping in mind that fungi and animals are both Opistokontha and comparable near relatives (compared to plants and fungi or animals and plants), we suggest that DHEA primarily interacts with the plasma membrane (Charalampopoulos et al., 2006; Lemcke et al., 2010).

All in all, our data indicate that DHEA is produced by infected plant tissues to fight fungal pathogens by attacking their membrane integrity. This can explain the high distribution of DHEA within the kingdom of plants. We could also show that this steroid enhances the leakage of plant cell membranes, too. Therefore, the accumulation of DHEA is a double-edgedsword and its metabolism has to be strictly regulated.

4. Conclusion

This study demonstrates that during fungal infection, *Arabidopsis thaliana* accumulates the C_{19}-steroid dehydroepiandrosterone (DHEA), a process localized to the infected plant organs. The effects of DHEA exhibit species-specific variations. In monocot species *Hordeum vulgare* and *Spirodela polyrhiza*, DHEA treatment led to increased salicylic acid levels, a response not observed in the dicot plant *A. thaliana*. Interestingly, while DHEA substantially affected root development in *A. thaliana*, this effect was absent in *H. vulgare*. At the transcriptome level, DHEA reduced the expression of membrane-associated genes in *A. thaliana*, indicating potential disruptions in cell and organelle membrane integrity. Moreover, DHEA inhibited the growth and spore production of the phytopathogenic fungus *Alternaria brassicicola*, although its ergosterol content remained unchanged, suggesting that the antifungal effect is likely due to disturbed fungal membranes.

Informed consent statement

Not applicable.

Institutional review board statement

Not applicable.

Author contribution

Conceptualization: J.K.; Method development instrumental analytics: C.M., F.F., and J.K; Investigation: C.O., G.S., M.L, F.F., S.M., K.L.K, H.L, A.A., R.O., M.R., K.O., A.C.U.F., and J.K.; Bioinformatic analysis: E. B., and J.K; Writing—original draft preparation: C.O., G.S., M.L., K.L.K., R.O., C.M., A.C.U.F., and J.K.; All authors have read and agreed to the published version of the manuscript.

Funding

This research was funded by IMPULSE^{project} (IP2022-13) of Friedrich Schiller University Jena.

Declaration of competing interest

The authors declare that they have no known competing financial interests or personal relationships that could have appeared to influence the work reported in this paper.

Acknowledgements

We thank **Franz Bracher** (Department of Pharmacy, Center for Drug Research, Ludwig-Maximilians-Universität München), **Jonathan Gershenzhon** (Department for Biochemistry, Max Planck Institute for Chemical Ecology) for providing laboratories and equipment. We thank **Klaus-Jürgen Appenroth** for the preparation of *Spirodela polyrhiza* clones, **Lilo Klein** and **Petra Sandjohann** for the preparation of *Hordeum vulgare* seeds. Thanks are due to **Svenja Tauber** of research group of bioactive plant products for lyophilizing our plant material. Big thanks to **Sandra Scholz** for preparing plant cultures and infections. Moreover, we thank **Hendrik Huthoff** and **Julie A. Z. Zedler** for helpful advice regarding manuscript editing.

Appendix A. Supplementary data

Supplementary data to this article can be found online at https://doi.org/10.1016/j.plaphy.2025.109570.

Data availability

Data is contained within the article or the supplement. Raw data of the RNAseq data are available on ncbi (Geo accession ID: GSE261582).

References

Al-Askar, A.A., Ghoneem, K.M., Rashad, Y.M., Abdulkhair, W.M., Hafez, E.E., Shabana, Y.M., Baka, Z.A., 2014. Occurrence and distribution of tomato seed-borne mycoflora in Saudi Arabia and its correlation with the climatic variables. Microb. Biotechnol. 7, 556–569.

Appenroth, K.-J., Teller, S., Horn, M., 1996. Photophysiology of turion formation and germination in *Spirodela polyrhiza*. Biologia plant 38.

Appenroth, K.-J., Sree, K.S., Bog, M., Ecker, J., Seeliger, C., Böhm, V., Lorkowski, S., Sommer, K., Vetter, W., Tolzin-Banasch, K., Kirmse, R., Leiterer, M., Dawczynski, C., Liebisch, G., Jahreis, G., 2018. Nutritional value of the duckweed species of the genus *wolffia* (Lemnaceae) as human food. Front. Chem. 6, 483.

Avery, S.V., Singleton, I., Magan, N., Goldman, G.H., 2019. The fungal threat to global food security. Fungal Biol. 123, 555–557.

Benjamini, Y., Hochberg, Y., 1995. Controlling the false discovery rate: a practical and powerful approach to multiple testing. J. Roy. Stat. Soc. B 57, 289–300.

Berardini, T.Z., Mundodi, S., Reiser, L., Huala, E., Garcia-Hernandez, M., Zhang, P., Mueller, L.A., Yoon, J., Doyle, A., Lander, G., Moseyko, N., Yoo, D., Xu, I., Zoeckler, B., Montoya, M., Miller, N., Weems, D., Rhee, S.Y., 2004. Functional annotation of the *Arabidopsis* genome using controlled vocabularies. Plant Physiol. 135, 745–755.

Botanga, C.J., Bethke, G., Chen, Z., Gallie, D.R., Fiehn, O., Glazebrook, J., 2012. Metabolite profiling of Arabidopsis inoculated with Alternaria brassicicola reveals that ascorbate reduces disease severity. Molecular plant-microbe interactions : MPMI (Mol. Plant-Microbe Interact.) 25, 1628–1638.

Brilhante, R.S.N., Oliveira, J.S. de, Jesus Evangelista, A.J. de, Pereira, V.S., Alencar, L.P., Castelo-Branco, D.d.S.C.M., Câmara, L.M.C., Lima-Neto, R.G. de, Cordeiro, R.d.A., Sidrim, J.J.C., Rocha, M.F.G., 2018. In vitro effects of promethazine on cell morphology and structure and mitochondrial activity of azole-resistant *Candida tropicalis*. Med. Mycol. 56, 1012–1022.

Caarls, L., Pieterse, C.M.J., van Wees, S.C.M., 2015. How salicylic acid takes transcriptional control over jasmonic acid signaling. Front. Plant Sci. 6, 170.

Camehl, I., Drzewiecki, C., Vadassery, J., Shahollari, B., Sherameti, I., Forzani, C., Munnik, T., Hirt, H., Oelmüller, R., 2011. The OXI1 kinase pathway mediates *Piriformospora indica*-induced growth promotion in *Arabidopsis*. PLoS Pathog. 7, e1002051.

Campoy, S., Adrio, J.L., 2017. Antifungals. Biochem. Pharmacol. 133, 86–96.

Carroll, E., Ravi Gopal, B., Raghavan, I., Mukherjee, M., Wang, Z.Q., 2023. A cytochrome P450 CYP87A4 imparts sterol side-chain cleavage in digoxin biosynthesis. Nat. Commun. 14, 4042.

Charalampopoulos, I., Alexaki, V.-I., Lazaridis, I., Dermitzaki, E., Avlonitis, N., Tsatsanis, C., Calogeropoulou, T., Margioris, A.N., Castanas, E., Gravanis, A., 2006. G protein-associated, specific membrane binding sites mediate the neuroprotective effect of dehydroepiandrosterone. FASEB journal : official publication of the Federation of American Societies for Experimental Biology 20, 577–579.

Chen, S., Zhou, Y., Chen, Y., Gu, J., 2018. fastp: an ultra-fast all-in-one FASTQ preprocessor. Bioinformatics 34, i884–i890.

Chomczynski, P., 1993. A reagent for the single-step simultaneous isolation of RNA, DNA and proteins from cell and tissue samples. Biotechniques 15 (532–4), 536–537.

Cvelbar, D., Zist, V., Kobal, K., Zigon, D., Zakelj-Mavrič, M., 2013. Steroid toxicity and detoxification in ascomycetous fungi. Chem. Biol. Interact. 202, 243–258.

Dovbnya, D.V., Egorova, O.V., Donova, M.V., 2010. Microbial side-chain degradation of ergosterol and its 3-substituted derivatives: a new route for obtaining of deltanoids. Steroids 75, 653–658.

Elsaman, H., Golubtsov, E., Brazil, S., Ng, N., Klugherz, I., Martin, R., Dichtl, K., Müller, C., Wagener, J., 2024. Toxic eburicol accumulation drives the antifungal activity of azoles against Aspergillus fumigatus. Nat. Commun. 15, 6312.

Fan, J., Du, N., Li, L., Li, G.-B., Wang, Y.-Q., Zhou, Y.-F., Hu, X.-H., Liu, J., Zhao, J.-Q., Li, Y., Huang, F., Wang, W.-M., 2019. A core effector UV_1261 promotes Ustilaginoidea virens infection via spatiotemporally suppressing plant defense. Phytopathology Research 1.

Fernández-Ortuño, D., Torés, J.A., Vicente, A. de, Pérez-García, A., 2008. Field resistance to QoI fungicides in *Podosphaera fusca* is not supported by typical mutations in the mitochondrial cytochrome b gene. Pest Manag. Sci. 64, 694–702.

Geißel, B., Loiko, V., Klugherz, I., Zhu, Z., Wagener, N., Kurzai, O., van den Hondel, C.A. M.J.J., Wagener, J., 2018. Azole-induced cell wall carbohydrate patches kill Aspergillus fumigatus. Nat. Commun. 9, 3098.

Genisel, M., Turk, H., Erdal, S., 2013. Exogenous progesterone application protects chickpea seedlings against chilling-induced oxidative stress. Acta Physiol. Plant. 35, 241–251.

Grigolli, J.F.J., Kubota, M.M., Alves, D.P., Rodrigues, G.B., Cardoso, C.R., Da Silva, D.J. H., Mizubuti, E.S.G., 2011. Characterization of tomato accessions for resistance to early blight. Crop Breed. Appl. Biotechnol. 11, 174–180.

Gsaller, F., Hortschansky, P., Furukawa, T., Carr, P.D., Rash, B., Capilla, J., Müller, C., Bracher, F., Bowyer, P., Haas, H., Brakhage, A.A., Bromley, M.J., 2016. Sterol biosynthesis and azole tolerance is governed by the opposing actions of SrbA and the CCAAT binding complex. PLoS Pathog. 12, e1005775.

Gupta, S.K., 2016. Brassicas. In: Breeding Oilseed Crops for Sustainable Production. Elsevier, pp. 33–53.

Hamsa, S., Rajarammohan, S., Aswal, M., Kumar, M., Kaur, J., 2024. Transcriptome responses of *Arabidopsis* to necrotrophic fungus *Alternaria brassicae* reveal pathways and candidate genes associated with resistance. Plant Mol. Biol. 114, 68.

Hao, J., Li, X., Xu, G., Huo, Y., Yang, H., 2019. Exogenous progesterone treatment alleviates chilling injury in postharvest banana fruit associated with induction of alternative oxidase and antioxidant defense. Food Chem. 286, 329–337.

Heyer, M., Reichelt, M., Mithöfer, A., 2018. A holistic approach to analyze systemic jasmonate accumulation in individual leaves of *Arabidopsis* rosettes upon wounding. Front. Plant Sci. 9, 1569.

Hosseini, P., Keniya, M.V., Sagatova, A.A., Toepfer, S., Müller, C., Tyndall, J.D.A., Klinger, A., Fleischer, E., Monk, B.C., 2024. The molecular basis of the intrinsic and acquired resistance to azole antifungals in Aspergillus fumigatus. Journal of Fungi 10, 820.

Janeczko, A., Tóbiás, I., Skoczowski, A., Dubert, F., Gullner, G., Barna, B., 2013. Progesterone moderates damage in *Arabidopsis thaliana* caused by infection with *Pseudomonas syringae* or *P. fluorescens*. Biologia plant. 57, 169–173.

Janeczko, A., 2021. Estrogens and androgens in plants: the last 20 Years of studies. Plants 10.

Jindo, K., Evenhuis, A., Kempenaar, C., Pombo Sudré, C., Zhan, X., Goitom Teklu, M., Kessel, G., 2021. Review: holistic pest management against early blight disease towards sustainable agriculture. Pest Manag. Sci. 77, 3871–3880.

Junker, J., Kamp, F., Winkler, E., Steiner, H., Bracher, F., Müller, C., 2021. Effective sample preparation procedure for the analysis of free neutral steroids, free steroid acids and sterol sulfates in different tissues by GC-MS. J. Steroid Biochem. Mol. Biol. 211, 105880.

Kámán-Tóth, E., Dankó, T., Gullner, G., Bozsó, Z., Palkovics, L., Pogány, M., 2019. Contribution of cell wall peroxidase- and NADPH oxidase-derived reactive oxygen species to *Alternaria brassicicola*-induced oxidative burst in Arabidopsis. Mol. Plant Pathol. 20, 485–499.

Kim, D., Paggi, J.M., Park, C., Bennett, C., Salzberg, S.L., 2019. Graph-based genome alignment and genotyping with HISAT2 and HISAT-genotype. Nat. Biotechnol. 37, 907–915.

Klein, J., 2024. Progesterone metabolism in *Digitalis* and other Plants - 60 years research and recent results. Plant Cell Physiol. https://doi.org/10.1093/pcp/pcae006.

Klein, J., Ernst, M., Christmann, A., Tropper, M., Leykauf, T., Kreis, W., Munkert, J., 2021a. Knockout of *Arabidopsis thaliana* VEP1, encoding a PRISE (progesterone 5β-reductase/iridoid synthase-like enzyme), leads to metabolic changes in response to exogenous methyl vinyl ketone (MVK). Metabolites 12.

Klein, J., Horn, E., Ernst, M., Leykauf, T., Leupold, T., Dorfner, M., Wolf, L., Ignatova, A., Kreis, W., Munkert, J., 2021b. RNAi-mediated gene knockdown of progesterone 5β-reductases in *Digitalis lanata* reduces 5β-cardenolide content. Plant Cell Rep. 40, 1631–1646.

Krauß, J., Müller, C., Klimt, M., Valero, L.J., Martínez, J.F., Müller, M., Bartel, K., Binder, U., Bracher, F., 2021. Synthesis, biological evaluation, and structure-activity relationships of 4-aminopiperidines as novel antifungal agents targeting ergosterol biosynthesis. Molecules 26.

Le Phuong, T., Fitrianti, A.N., Luan, M.T., Matsui, H., Noutoshi, Y., Yamamoto, M., Ichinose, Y., Shiraishi, T., Toyoda, K., 2020. Antagonism between SA- and JA-signaling conditioned by saccharin in Arabidopsis thaliana renders resistance to a specific pathogen. J. Gen. Plant Pathol. 86, 86–99.

Lemcke, S., Hönnscheidt, C., Waschatko, G., Bopp, A., Lütjohann, D., Bertram, N., Gehrig-Burger, K., 2010. DHEA-Bodipy–a functional fluorescent DHEA analog for live cell imaging. Mol. Cell. Endocrinol. 314, 31–40.

Li, H., Handsaker, B., Wysoker, A., Fennell, T., Ruan, J., Homer, N., Marth, G., Abecasis, G., Durbin, R., 2009. The sequence alignment/map format and SAMtools. Bioinformatics 25, 2078–2079. Oxford, England.

Liao, Y., Smyth, G.K., Shi, W., 2014. featureCounts: an efficient general purpose program for assigning sequence reads to genomic features. Bioinformatics 30, 923–930.

Liebl, M., Huber, L., Elsaman, H., Merschak, P., Wagener, J., Gsaller, F., Müller, C., 2023. Quantifying isoprenoids in the ergosterol biosynthesis by gas chromatography-mass spectrometry. Journal of fungi (Basel, Switzerland) 9.

Liu, L., Wang, D., Li, L., Ding, X., Ma, H., 2016. Dehydroepiandrosterone inhibits cell proliferation and improves viability by regulating S phase and mitochondrial permeability in primary rat Leydig cells. Mol. Med. Rep. 14, 705–714.

Livak, K.J., Schmittgen, T.D., 2001. Analysis of relative gene expression data using real-time quantitative PCR and the 2(-Delta Delta C(T)) Method. Methods (San Diego, Calif.) 25, 402–408.

Love, M.I., Huber, W., Anders, S., 2014. Moderated estimation of fold change and dispersion for RNA-seq data with DESeq2. Genome biology 15, 550.

McKinney, W., 2010. Data structures for statistical computing in Python. In: Proceedings of the 9th Python in Science Conference. Python in Science Conference. SciPy, pp. 56–61. Austin, Texas. June 28 - July 3 2010.

Müller, C., Binder, U., Bracher, F., Giera, M., 2017. Antifungal drug testing by combining minimal inhibitory concentration testing with target identification by gas chromatography-mass spectrometry. Nat. Protoc. 12, 947–963.

Müller, C., Neugebauer, T., Zill, P., Lass-Flörl, C., Bracher, F., Binder, U., 2018. Sterol composition of clinically relevant mucorales and changes resulting from posaconazole treatment. Molecules 23.
Müller, C., Staudacher, V., Krauss, J., Giera, M., Bracher, F., 2013. A convenient cellular assay for the identification of the molecular target of ergosterol biosynthesis inhibitors and quantification of their effects on total ergosterol biosynthesis. Steroids 78, 483–493.
Murashige, T., Skoog, F., 1962. A revised medium for rapid growth and bio assays with tobacco tissue cultures. Physiol. Plantarum 15, 473–497.
Neunzig, J., Sánchez-Guijo, A., Mosa, A., Hartmann, M.F., Geyer, J., Wudy, S.A., Bernhardt, R., 2014. A steroidogenic pathway for sulfonated steroids: the metabolism of pregnenolone sulfate. The Journal of steroid biochemistry and molecular biology 144 Pt B, 324–333.
Nottensteiner, M., Absmeier, C., Zellner, M., 2019. QoI fungicide resistance mutations in *Alternaria solani* and *Alternaria alternata* are fully established in potato growing areas in bavaria and dual resistance against SDHI fungicides is upcoming. Gesunde Pflanz. 71, 155–164.
Nowakowska, M., Wrzesińska, M., Kamiński, P., Szczechura, W., Lichocka, M., Tartanus, M., Kozik, E.U., Nowicki, M., 2019. *Alternaria brassicicola* – brassicaceae pathosystem: insights into the infection process and resistance mechanisms under optimized artificial bio-assay. Eur. J. Plant Pathol. 153, 131–151.
Nowicki, M., Nowakowska, M., Niezgoda, A., Kozik, E., 2012. *Alternaria* black spot of crucifers: symptoms, importance of disease, and perspectives of resistance breeding. J. Fruit Ornam. Plant Res. 76, 5–19.
Ntow-Boahene, W., Papandronicou, I., Miculob, J., Good, L., 2023. Fungal cell barriers and organelles are disrupted by polyhexamethylene biguanide (PHMB). Sci. Rep. 13, 2790.
Pinto, V.E.F., Patriarca, A., 2017. Alternaria species and their associated mycotoxins. Methods Mol. Biol. 1542, 13–32.
Polisensky, D.H., Braam, J., 1996. Cold-shock regulation of the *Arabidopsis* TCH genes and the effects of modulating intracellular calcium levels. Plant Physiol. 111, 1271–1279.
Poojary, S., 2017. Topical antifungals: a review and their role in current management of dermatophytoses. Clin Dermatol Rev 1, 24.
Rentel, M.C., Knight, M.R., 2004. Oxidative stress-induced calcium signaling in *Arabidopsis*. Plant Physiol. 135, 1471–1479.
Rocher, F., Chollet, J.-F., Jousse, C., Bonnemain, J.-L., 2006. Salicylic acid, an ambimobile molecule exhibiting a high ability to accumulate in the phloem. Plant Physiol. 141, 1684–1693.
Rocher, F., Chollet, J.-F., Legros, S., Jousse, C., Lemoine, R., Faucher, M., Bush, D.R., Bonnemain, J.-L., 2009. Salicylic acid transport in Ricinus communis involves a pH-dependent carrier system in addition to diffusion. Plant Physiol. 150, 2081–2091.
Rotem, J., 1998. The Genus *Alternaria*: Biology, Epidemiology, and Pathogenicity. APS Press, St. Paul, Minn, p. 326.
Sabzmeydani, E., Sedaghathoor, S., Hashemabadi, D., 2020. Progesterone and salicylic acid elevate tolerance of poa pratensis to salinity stress. Russ. J. Plant Physiol. 67, 285–293.
Schanzer, S., Koch, M., Kiefer, A., Jentke, T., Veith, M., Bracher, F., Bracher, J., Müller, C., 2022. Analysis of pesticide and persistent organic pollutant residues in German bats. Chemosphere 305, 135342.
Schanzer, S., Kröner, E., Wibbelt, G., Koch, M., Kiefer, A., Bracher, F., Müller, C., 2021. Miniaturized multiresidue method for the analysis of pesticides and persistent organic pollutants in non-target wildlife animal liver tissues using GC-MS/MS. Chemosphere 279, 130434.
Schiffer, L., Brixius-Anderko, S., Hannemann, F., Zapp, J., Neunzig, J., Thevis, M., Bernhardt, R., 2016. Metabolism of oral turinabol by human steroid hormone-synthesizing cytochrome P450 enzymes. Drug Metabol. Dispos.: the biological fate of chemicals 44, 227–237.
Schuhegger, R., Rauhut, T., Glawischnig, E., 2007. Regulatory variability of camalexin biosynthesis. J. Plant Physiol. 164, 636–644.
Shen, X., Liu, L., Yin, F., Ma, H., Zou, S., 2012. Effect of dehydroepiandrosterone on cell growth and mitochondrial function in TM-3 cells. Gen. Comp. Endocrinol. 177, 177–186.
Shiko, G., Paulmann, M.-J., Feistel, F., Ntefidou, M., Hermann-Ene, V., Vetter, W., Kost, B., Kunert, G., Zedler, J.A.Z., Reichelt, M., Oelmüller, R., Klein, J., 2023. Occurrence and conversion of progestogens and androgens are conserved in land plants. New Phytol. 240, 318–337.
Shpakovski, G.V., Spivak, S.G., Berdichevets, I.N., Babak, O.G., Kubrak, S.V., Kilchevsky, A.V., Aralov, A.V., Slovokhotov, I.Y., Shpakovski, D.G., Baranova, E.N., Khaliluev, M.R., Shematorova, E.K., 2017. A key enzyme of animal steroidogenesis can function in plants enhancing their immunity and accelerating the processes of growth and development. BMC Plant Biol. 17, 189.
Simons, R.G., Grinwich, D.L., 1989. Immunoreactive detection of four mammalian steroids in plants. Can. J. Bot. 67, 288–296.
Stukenbrock, E.H., McDonald, B.A., 2008. The origins of plant pathogens in agro-ecosystems. Annu. Rev. Phytopathol. 46, 75–100.
Suchodolski, J., Muraszko, J., Bernat, P., Krasowska, A., 2019. A crucial role for ergosterol in plasma membrane composition, localisation, and activity of Cdr1p and H+-ATPase in Candida albicans. Microorganisms 7.
Vadassery, J., Ranf, S., Drzewiecki, C., Mithöfer, A., Mazars, C., Scheel, D., Lee, J., Oelmüller, R., 2009. A cell wall extract from the endophytic fungus *Piriformospora indica* promotes growth of *Arabidopsis* seedlings and induces intracellular calcium elevation in roots. Plant J. : for cell and molecular biology 59, 193–206.
Venkateswarlu, K., Kelly, S.L., 1996. Biochemical characterisation of ketoconazole inhibitory action on *Aspergillus fumigatus*. FEMS Immunol. Med. Microbiol. 16, 11–20.
Weete, J.D., Abril, M., Blackwell, M., 2010. Phylogenetic distribution of fungal sterols. PLoS One 5, e10899.
Wolf, J., O'Neill, N.R., Rogers, C.A., Muilenberg, M.L., Ziska, L.H., 2010. Elevated atmospheric carbon dioxide concentrations amplify *Alternaria alternata* sporulation and total antigen production. Environ. Health Perspect. 118, 1223–1228.
Zhang, S., Miao, W., Liu, Y., Jiang, J., Chen, S., Chen, F., Guan, Z., 2023. Jasmonate signaling drives defense responses against Alternaria alternata in chrysanthemum. BMC Genom. 24, 553.
Zhang, Z., Gao, B., He, Z., Li, L., Zhang, Q., Kaziem, A.E., Wang, M., 2019. Stereoselective bioactivity of the chiral triazole fungicide prothioconazole and its metabolite. Pestic. Biochem. Physiol. 160, 112–118.
Zinser, E., Paltauf, F., Daum, G., 1993. Sterol composition of yeast organelle membranes and subcellular distribution of enzymes involved in sterol metabolism. J. Bacteriol. 175, 2853–2858.